Molecular Biology of the Cell
Vol. 8, 1481–1499, August 1997

Yeast Actin Cytoskeleton Mutants Accumulate a New Class of Golgi-derived Secretory Vesicle

Jon Mulholland,* Andreas Wesp,† Howard Riezman,† and David Botstein*‡

*Department of Genetics, Stanford University Medical School, Stanford California 94305; and
†Biozentrum of the University of Basel, Klingelbergstrasse 70, CH-4056, Switzerland

Submitted November 21, 1996; Accepted May 1, 1997
Monitoring Editor: Randy Schekman

Many yeast actin cytoskeleton mutants accumulate large secretory vesicles and exhibit phenotypes consistent with defects in polarized growth. This, together with actin's polarized organization, has suggested a role for the actin cytoskeleton in the vectorial transport of late secretory vesicles to the plasma membrane. By using ultrastructural and biochemical analysis, we have characterized defects manifested by mutations in the *SLA2* gene (also known as the *END4* gene), previously found to affect both the organization of the actin cytoskeleton and endocytosis in yeast. Defects in cell wall morphology, accumulated vesicles, and protein secretion kinetics were found in *sla2* mutants similar to defects found in *act1* mutants. Vesicles that accumulate in the *sla2* and *act1* mutants are immunoreactive with antibodies directed against the small GTPase Ypt1p but not with antibodies directed against the homologous Sec4p found on classical "late" secretory vesicles. In contrast, the late-acting secretory mutants *sec1–1* and *sec6–4* are shown to accumulate anti-Sec4p–positive secretory vesicles as well as vesicles that are immunoreactive with antibodies directed against Ypt1p. The late *sec* mutant *sec4–8* is also shown to accumulate Ypt1p-containing vesicles and to exhibit defects in actin cytoskeleton organization. These results indicate the existence of at least two classes of morphologically similar, late secretory vesicles (associated with $Ypt1p^+$ and $Sec4p^+$, respectively), one of which appears to accumulate when the actin cytoskeleton is disorganized.

INTRODUCTION

Studies of the functions of the actin cytoskeleton in budding yeast (*Saccharomyces cerevisiae*) have pointed to roles in polarized growth and protein secretion. Mutants defective in the structural gene encoding yeast actin (*act1* mutants) display characteristic defects in cell morphology, in the kinetics of protein secretion, and accumulate intracellular membranous structures, including vesicles (reviewed in Welch *et al.*, 1994; Botstein *et al.*, 1997).

The organization of the actin cytoskeleton, as observed by immunofluorescence and immunoelectron microscopy (immuno-EM), is entirely consonant with this view of actin function. The yeast actin cytoskeleton consists of two major structures, cables and cortical patches (Adams and Pringle, 1984; Kilmartin and Adams, 1984; Novick and Botstein, 1985; Read *et al.*, 1992; Mulholland *et al.*, 1994). These structures are asymmetrically organized along the axis of cell growth throughout the cell cycle. Cortical actin patches are concentrated in areas of active cell surface growth within the bud for most of the cell cycle and at the septum during cytokinesis. Actin cables are localized within both the mother and bud and are oriented along the mother–daughter cell axis.

The actin cytoskeleton contains proteins other than actin itself. Many of these proteins have been identified, some by genetic methods, some by biochemical methods, some by homologies to proteins known to bind actin in other organisms, and some by use of the two-hybrid system for detecting protein interactions (reviewed in Botstein *et al.*, 1997). The phenotypes of mutants defective in the genes specifying these actin-associated proteins tend to be similar to at least some aspects of the *act1* mutant phenotypes, particularly with respect to loss of cell polarity.

‡ Corresponding author.

Surprisingly, deletion of the gene encoding the actin-binding protein *ABP1* does not produce a detectable phenotype (Drubin *et al.*, 1988). However, null mutations in this gene show synthetic lethality with null mutations in another gene (*SAC6*) encoding an actin binding protein related to fimbrin (Adams *et al.*, 1989, 1991). Genetic screening for mutations in other genes that display synthetic lethality with *abp1* mutations, resulted in the recovery of two new genes, *SLA1* and *SLA2* (Holtzman *et al.*, 1993). Although neither of these genes is essential, deletion of either gene produces defects in the organization of the actin cytoskeleton and in cell polarity (Holtzman *et al.*, 1993).

Secretion-defective mutations, especially those affecting the transit of proteins from the Golgi to the plasma membrane (e.g., *sec4*, *sec1*, or *sec6*), often show accumulation of a uniform class of large vesicles (Novick *et al.*, 1980, 1981). In wild-type cells, these vesicles contain on their cytoplasmic surface Sec4p, a small GTPase of the Ras family that is involved mediating vesicle fusion to the plasma membrane (Salminen and Novick, 1987; Goud *et al.*, 1988; Walworth *et al.*, 1992). Such vesicles are seen in wild-type cells only in very small buds, near the septum at cytokinesis, and in shmoo tips—all sites of active membrane growth. Actin mutants and many of the actin cytoskeleton mutants also accumulate apparently similar large vesicles. Further, actin mutants have defects in protein secretion analogous to those manifested by the late-acting secretory mutants. Together with the polarized organization of the actin cytoskeleton, these observations implicated actin in the vectorial transport of late secretory vesicles to the plasma membrane.

The argument for actin's involvement in membrane traffic has been buttressed further by the finding that some *act1* mutants and *sac6* null mutants (but not *abp1* null mutants) are defective in receptor-mediated endocytosis (Kubler and Riezman, 1993). Phenotypic screening for endocytosis mutants identified *END4*, a gene required for both receptor-mediated and fluid-phase endocytosis (Raths *et al.*, 1993; Munn *et al.*, 1995). Upon DNA sequencing, *SLA2* and *END4* turned out to be the same gene. This same gene was found in a third genetic screen for enhancers of the mutant phenotype of mutations in the *PMA1* gene, which encodes the yeast plasma membrane proton ATPase (Na *et al.*, 1995).

To clarify the connection between the actin cytoskeleton and membrane trafficking in yeast, we have characterized the defects manifested by *sla2* and *act1* mutants by using both immuno-EM and biochemical analysis. In the course of this study, we have found a new class of large secretory vesicle containing Ypt1p in place of Sec4p. These Ypt1p-associated vesicles accumulate when the actin cytoskeleton is perturbed.

MATERIALS AND METHODS

Yeast Strains and Growth Conditions

The yeast strains used in this study are listed in Table 1; all strains listed are direct descendants of strain S288C. Standard genetic techniques including growth, crosses, sporulation, tetrad analysis, and complementation tests were done as described in Guthrie and Fink (1991) and Kaiser *et al.* (1994).

For metabolic labeling experiments yeast strains were grown in SDYE [0.67% yeast nitrogen base (Difco, Detroit, MI), 0.2% Bacto yeast extract (Life Technologies, Paisley, Scotland)], 2% glucose supplemented with 20 mg/ml adenine, 20 mg/ml histidine, 20 mg/ml uracil, 20 mg/ml tryptophan, 20 mg/ml lysine, 20 mg/ml leucine, and 20 mg/ml tyrosine (E. Merck, Darmstadt, Germany). YNB is SDYE without yeast extract.

For immuno-EM, strains were grown at either the permissive temperature 25°C or grown at 25°C and then shifted to the restrictive temperature 37°C in yeast-extract peptone medium (YEP; Sherman *et al.*, 1986) containing 2% glucose. Cell cultures were harvested for immuno-EM at a cell density of between 0.4 and 0.6 OD_{600}. All cells were fixed and processed for immuno-EM as described below.

Metabolic Labeling and Immunoprecipitations

Cells were grown in SDYE at 24°C to a density of 0.9–1.2 × 10^7 cells/ml, and 5 × 10^7 cells per time point were harvested by centrifugation at 2000 rpm in a GLC centrifuge (Sorvall, Wilmington, DE, General Laboratory Centrifuge). Cells were washed in 20 ml of YNB and resuspended to a concentration of 10^8 cells/ml in YNB. Cells were then transferred to 50-ml Falcon tubes and preincubated, in a rotary water shaker at either 24°C or 37°C, for 15 min. One hundred microcuries of Express Protein Labeling mixture (New England Nuclear, Du Pont, Germany) per time point were added and incubation was continued for 5 more min. Chase was then initiated by adding 100× chase solution [0.3% cysteine, 0.3% methionine, 0.3 M $(NH4)_2SO_4$]. Culture medium (0.4 ml of medium per time) was harvested at 0, 5, 15, and 30 min after initiating the chase

Table 1. Yeast strains

Strain	Genotype
RH448[a]	*MATa his4 leu2 ura3 lys2 bar1-1*
RH1597[a]	*MATa sla2-41 his4 leu2 ura3 bar1-1*
RH3212[a]	*MATa sla2Δ2* his3 leu2 ura3 lys2 trp1 bar1-1*
DBY2061	*MATa ura3-52 leu2-3,112*
DBY5907[b]	*MATa sla2-5 leu2-3,112 ura3-52*
DBY5908[b]	*MATα sla2Δ1* leu2-3,112 ura3-52*
DBY1691	*MATa his4-619 act1-1*
DBY1695	*MATa his4-619 act1-2*
DBY6550[c]	*MATα sec12-4 ura3-52 leu2-3,112*
DBY6552[c]	*MATα sla2-5 sec12-4 ura3-52 leu2-3,112*
DBY6538[c]	*MATα sec17-1 ura3-52 his4-619*
DBY6540[c]	*MATα sla2-5 sec17-1 ura3-52*
DBY5888[d]	*MATa sec1-1 ura3-52*
DBY5894[d]	*MATa sec4-8 ura3-52*
DBY5889[d]	*MATa sec6-4 ura3-52*

[a] From Howard Riezman (Biozentrum, Basel, Switzerland).

[b] From David Drubin (University of California, Berkeley).

[c] This study.

[d] From Chris Kaiser (Massachusetts Institute of Technology, Cambridge, MA).

* *sla2Δ1* is *sla2*::URA3 and *sla2Δ2* is *sla*::HIS3

and transferred into Eppendorf tubes (on ice) containing NaF and NaN_3 at a final concentration of 25 mM.

For immunoisolation of CPY, cells were spun down in a microcentrifuge and the supernatant was discarded. Cells were resuspended in 0.44 ml of phosphate-buffered saline (PBS: 0.1 M NaCl, 80 mM Na_2HPO_4, 20 mM NaH_2PO_4) and 1% SDS containing protease inhibitor mixture (antipain, leupeptin, pepstatin, each at a final concentration of 1 μg/ml, phenylmethylsulfonyl fluoride at 1 mM final concentration) and 0.2 g of acid-washed glass beads were added. Samples were vortexed four times consecutively at maximum setting for 1 min with an incubation on ice between each. Samples were boiled for 5 min and supernatants were then transferred to a fresh Eppendorf tube. Glass beads, washed with 1.32 ml of PBS and 1.33% Triton X-100 (TX-100) were added to the lysate. Particulate material was removed by centrifugation for 10 min at 13,000 rpm in a microcentrifuge and supernatants were transferred to new tubes. Rabbit anti-CPY polyclonal antibodies (Schimmoller *et al.*, 1995) were added and incubated for 90 min at room temperature (RT). Then, 50 μl of 30% protein A-Sepharose in PBS were added and incubation was continued for another 60 min at RT. The protein A-Sepharose beads were then recovered by centrifugation and transferred in 0.5 ml of PBS and 1% TX-100 to new tubes. Beads were washed twice in the same buffer, transferred in 10 mM Tris-HCl (pH 7.5), and 10 mM NaCl to new tubes, and finally resuspended in 60 μl of 2× sample buffer [4% SDS, 4% 2-mercaptoethanol, 20% glycerol, 125 mM Tris-HCl, pH 6.8, 0.02% bromophenol blue]. Samples were subsequently boiled for 5 min, beads were spun down, and 45 μl of the supernatant were loaded onto SDS-7.5% polyacrylamide gels to separate immunoprecipitated proteins. Gels were fixed in 30% ethanol and 10% acetic acid, dried onto Whatman paper, and exposed to XAR X-ray films (Kodak, Rochester, NY).

Maturation of Gas1p was followed similarly by using the same immunoprecipitation protocol except that rabbit anti-Gas1p polyclonal antibodies (Schimmoller *et al.*, 1995) were used. Gels were exposed to Storage Phosphor Screen (Molecular Dynamics, Sunnyvale, CA) and visualized with the Image Quant V3.2 software (Molecular Dynamics).

To follow maturation and secretion of invertase, cells were grown in SDYE at 24°C and then converted to spheroplasts in buffer containing 0.1% glucose, essentially as described in Schimmoller *et al.* (1993). Spheroplasts were harvested by centrifugation at 1500 rpm in a GLC centrifuge; washed twice in 10 ml of YNB, 0.1% glucose, and 0.8 M sorbitol; and resuspended to a concentration of 10^8 cells/ml in YNB, 0.1% glucose, and 0.8 M sorbitol. The spheroplasts were then transferred to 50-ml Falcon tubes and preincubated at either 24°C or 37°C for 15 min in a rotary water shaker. Protein-label mixture was subsequently added as described above and spheroplasts were incubated for 4 more min. The chase was initiated as described above and 0.4 ml of culture medium was removed at 0, 5, 15, and 30 min after initiating the chase and transferred into Eppendorf tubes on ice containing NaF and NaN_3 at a final concentration of 25 mM. Cells were spun down; supernatants were transferred to new tubes. To the transferred supernatant fractions, 44 μl of 10% SDS were added while the cell fractions were resuspended in 440 μl of PBS and 1% SDS. All samples were boiled for 5 min and then spun for 10 min at 13,000 rpm in a microcentrifuge to remove all remaining particulate material. Supernatants were transferred to new tubes and 1.32 ml of PBS and 1.33% TX-100 was added to all samples. Anti-invertase polyclonal rabbit antibodies (Schimmoller *et al.*, 1995) were then added and samples were processed as described above.

Fixation and Processing for Immuno-EM

Fixation and processing of yeast cells was done as described in Mulholland *et al.* (1994) except for the following change in fixation conditions. The buffered fixative used in this study was 40 mM potassium phosphate, pH 6.7, 0.8 M sorbitol, and 4% formaldehyde freshly prepared from paraformaldehyde (Polysciences, Warrington, PA), 0.4% glutaraldehyde (EM grade, Polysciences), 1 mM $MgCl_2$, and 1 mM EGTA. This fixative has a lower osmotic strength than our standard fixative. Use of a lower osmotic strength fixative was necessary because fixation at our standard osmotic strength (provided by 1 M sorbitol) produced plasmolysis in the *act1* mutants. This was particularly noticeable in mutant cells grown at 37°C.

Ultramicrotomy, Immunolabeling, and Electron Microscopy

Thin sections measuring 60–70 nm (as determined by a gray/silver interference color) were cut with a 35° diamond knife (Diatome, Fort Washington, PA) and were picked up on 300-mesh nickel grids (Polysciences) that had been made sticky with a dilute Formvar solution (Wright and Rine, 1989).

Production, purification, and characterization of affinity-purified polyclonal rabbit antibodies raised against TrpE-Ypt1p and TrpE-Sec4p fusion proteins have been described previously (Goud *et al.*, 1988; Segev *et al.*, 1988). The specificity of the rabbit anti-α-1,6-mannose antisera preparation has been previously demonstrated (Franzusoff and Schekman, 1989; Preuss *et al.*, 1992). Antibody incubations were performed as described previously (Mulholland, *et al.*, 1994). All antibodies were diluted in PBST (140 mM NaCl, 3 mM KCl, 8 mM Na_2HPO_4, 1.5 mM KH_2PO_4, 0.05% Tween 20) containing 0.5% bovine serum albumin and 0.5% ovalbumin (Sigma, St. Louis, MO) and were incubated with cell sections mounted on grids as described above. Anti-Ypt1p antibodies were diluted 1:30, anti-Sec4p antibodies were diluted 1:30, and anti-α-1,6-mannose antisera was diluted 1:80,000. The 10-nm-gold–conjugated anti-rabbit IgG (goat) secondary antibodies (BioCell, Cardiff, United Kingdom) were all diluted 1:50 in PBST, 0.5% bovine serum albumin, and 0.5% ovalbumin. In the absence of the primary antibody the anti-rabbit secondary antibodies did not react with the cell sections.

Following immunolocalization, cell sections were postfixed in 8% glutaraldehyde (EM grade, Polysciences) and stained with uranyl acetate and lead citrate as previously described (Mulholland *et al.*, 1994). All observations were made on a Phillips 300 EM at an accelerating voltage of 80 kV using a 20-μm-diameter objective aperture.

α-Factor Treatment of Wild-Type and sla2 Cells

Wild-type (RH448) and *sla2–41* (RH1597) cell cultures were grown at 25°C in YPD (2%) medium to an OD_{600} of approximately 0.3 and then α-factor (Sigma, St. Louis, MO) was added to a concentration of 2.5 μM (Sprague, 1991). Immediately after the addition of α-factor, the cultures were split and one half of each culture remained at 25°C and the other half was incubated at 37°C. Samples were then taken from both cultures at 0, 15, 30, 60, and 90 min following the addition of α-factor and immediately fixed and processed for immuno-EM as described above.

G_1 arrest and shmooing (formation of a pear-shaped cell morphology) was monitored with phase-contrast light microscopy. The degree of shmoo formation in wild-type and *sla2* mutant cultures was quantitatively similar at 37°C, at all time points observed. After 1.5 h at 37°C, approximately 50% of all cells observed in both the wild-type and mutant cell cultures had formed shmoos. Cell sections from the 60-min time point were used in the immuno-EM experiments described.

Phalloidin Staining of the Actin Cytoskeleton

Wild-type and *sec4–8* cells, growing at 25°C or incubated at 36°C for 30 and 60 min, were fixed by direct addition of an equal volume of methanol-free 10% formaldehyde (Polysciences). After an initial 10-min fixation at culture temperature (25°C or 36°C), cells were collected by centrifugation and resuspended in 4% formaldehyde and incubated at RT for 1 h. Cells were then washed three times in

PBS and resuspended in 0.5 ml of PBS. Subsequent processing for rhodamine-phalloidin fluorescence light microscopy was according to Pringle *et al.* (1989).

RESULTS

sla2 Mutants Exhibit Defects in Wall Deposition

To determine whether *sla2* mutants exhibited any ultrastructural phenotypes indicative of defects in secretion and cell surface growth, cultures of the deletion strains *sla2Δ1* and *sla2Δ2* and the point mutation strains *sla2–5* and *sla2–41* were fixed, sectioned, stained, and examined in the electron microscope. This examination of the *sla2* mutants revealed a characteristic aberrant cell wall morphology. About half of all mutant mother cells observed had cell walls that were thicker than the wild-type cell wall and these thicker walls often appeared to consist of several distinct layers, each with a thickness about that of a normal cell wall (Figure 1).

In contrast, all growing buds, including large buds that had finished septation but were still attached to their mother cells exhibited wild-type wall morphology. In all budded cells observed, the inner plasma membrane-associated wall on the mother cell was continuous with the new wall of the bud. Often, the outer wall(s) of the mother cell appeared to have been torn open at the site of bud emergence (Figure 1, B and C). Similar defects in wall ultrastructure were observed in cells from both the *sla2* deletion and point mutation strains.

Consistent with defects in cell wall deposition, defects in septum morphology also were observed in the *sla2* mutants. Examination of mutant cells undergoing cytokinesis often revealed inclusions of cytoplasm within the septum wall (Figure 1D). These wall and septum abnormalities were observed to the same extent at both the permissive and nonpermissive temperatures, indicating a constitutive temperature-independent defect.

Examination of *act1–1* mutant cells at both permissive (25°C) and restrictive (37°C) temperature revealed aberrant morphology of the cell wall and septum (Figure 1, E and F). These defects were identical to those observed in the *sla2* mutants.

sla2 Mutants Accumulate Large Vesicles that Do Not Contain Sec4p

Besides the obvious cell wall and septum defects, examination of the *sla2* mutants revealed a polarized accumulation of large vesicles (40–60 nm) (see Figures 1 through 5 for examples). Although all of the mutant strains (including the *sla2* deletions) have temperature-sensitive lethal growth phenotypes, polarized accumulation of vesicles was seen at both permissive (25°C) and nonpermissive (37°C) temperatures. However, the accumulation of vesicles was more extensive at the nonpermissive temperature. At all temperatures, the vesicles accumulated at the base of small buds and within buds of all sizes. Though some vesicles were observed in mother cells, the majority of vesicles, even after 1.5 h at the nonpermissive temperature, were concentrated within the growing bud or at the site of septum formation. Within the bud, accumulated vesicles frequently appeared to be randomly dispersed. In contrast, vesicles observed at the base of the neck of small budded cells as well at the tip of larger buds were aggregated into dense clusters.

Late *sec* mutants (e.g., *sec1–1*, *sec4–8*) also accumulate large secretory vesicles (Novick *et al.*, 1980, 1981) and these vesicles appear to be similar in size and morphology to the vesicles that accumulate in *sla2* mutants. Thus, it seemed reasonable to hypothesize that the *sla2* mutants might accumulate secretory vesicles at a point in the secretory pathway similar to that of the late secretory mutants. Sec4p is a small GTPase involved in mediating fusion of late secretory vesicles to the yeast plasma membrane and immunofluorescence light microscopy studies have shown that Sec4p is located at areas of active cell surface growth (Salminen and Novick, 1987; Goud *et al.*, 1988; Walworth *et al.*, 1992). Furthermore, Sec4p has been shown to be associated with late secretory vesicles purified from several different late *sec* mutants (Goud *et al.*, 1988). To test whether vesicles accumulate in the *sla2* mutants at a step analogous to late secretory mutants, we conducted immuno-EM experiments using affinity-purified antibodies directed against Sec4p (see MATERIALS AND METHODS).

Because immunolocalization of Sec4p to secretory vesicles in vivo had not been demonstrated directly, we first characterized Sec4p localization on sections of wild-type cells. As expected, immuno-EM on wild-type cell sections located Sec4p to the large secretory vesicles concentrated at areas of active cell growth (Figure 2). Specifically, anti-Sec4p antibodies localized to the secretory vesicles that filled small buds (Figure 2, A and B) as well as to vesicles located along the plasma membrane at the tip of larger buds. Sec4p antibodies also labeled secretory vesicles at the site of septum formation.

In the *sla2* mutant cells grown at 25°C or incubated at 37°C, almost no Sec4p localization was observed on the 40- to 60-nm vesicles that accumulated in growing buds and no Sec4p localization was observed on the clusters of vesicles. Figure 2, C–D, shows examples taken from samples incubated at 37°C. The vast majority of the large vesicles that accumulated in these mutants appear not to contain much, if any, Sec4p, suggesting that the defect in the mutants causes failure of a step(s) prior to the Sec4p-mediated fusion with the plasma membrane. It should be noted that an

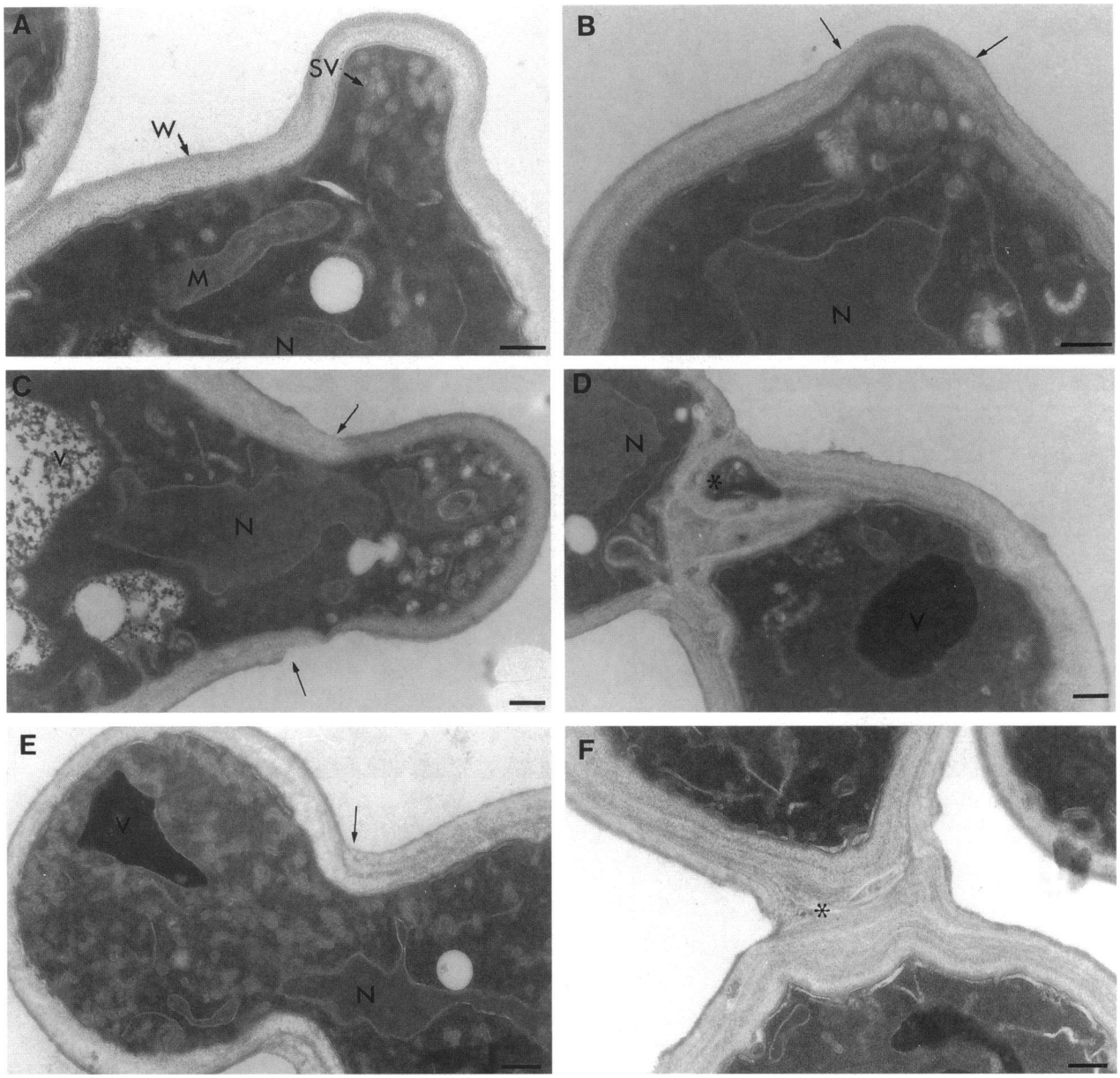

Figure 1. *sla2* and *act1* mutants have aberrant cell wall morphology. (A) Wild-type (RH448) cell grown at 25°C. (B) Emerging bud of a *sla2–41* (RH1597) cell grown at 25°C; note the double-layered cell wall on the mother and the continuity between the single-cell wall layer in the bud with the inner layer of the mother. (C) *sla2–41* cells grown at 37°C for 1.5 h. (D) Septation defects in the *sla2–41* cells at 37°C. *, Large cytoplasmic inclusion. Cells shown in D are two double-walled mother cells of a three-cell chain. (E and F) *act1–1* mutant incubated at 37°C for 1 h; note bud filled with large vesicles and characteristic double wall in mother (arrow). (F) Two *act1–1* mother cells of a three cell chain; note multiple wall and septum defects. Thin arrows in B, C, and E point to transition from multiple to single wall. G, Golgi; M, mitochondria; N, nucleus; SV, secretory vesicles; V, vacuole; W, wall. Bars, 0.25 μm.

occasional bud or septum could be found to contain vesicles that labeled with antibodies against Sec4p, but this labeling was never as heavy as that observed in wild-type buds, suggesting that residual Sec4p-associated secretory vesicles are present and properly localized in the *sla2* mutant strains.

Vesicles that Accumulate in sla2 Mutants Contain α-1,6-Mannose Residues and Ypt1p

Previously, Pruess *et al.* (1992) showed that early in the yeast cell cycle Golgi membranes are invariably positioned at the base of the neck of small buds and that these Golgi membranes are segregated into the growing

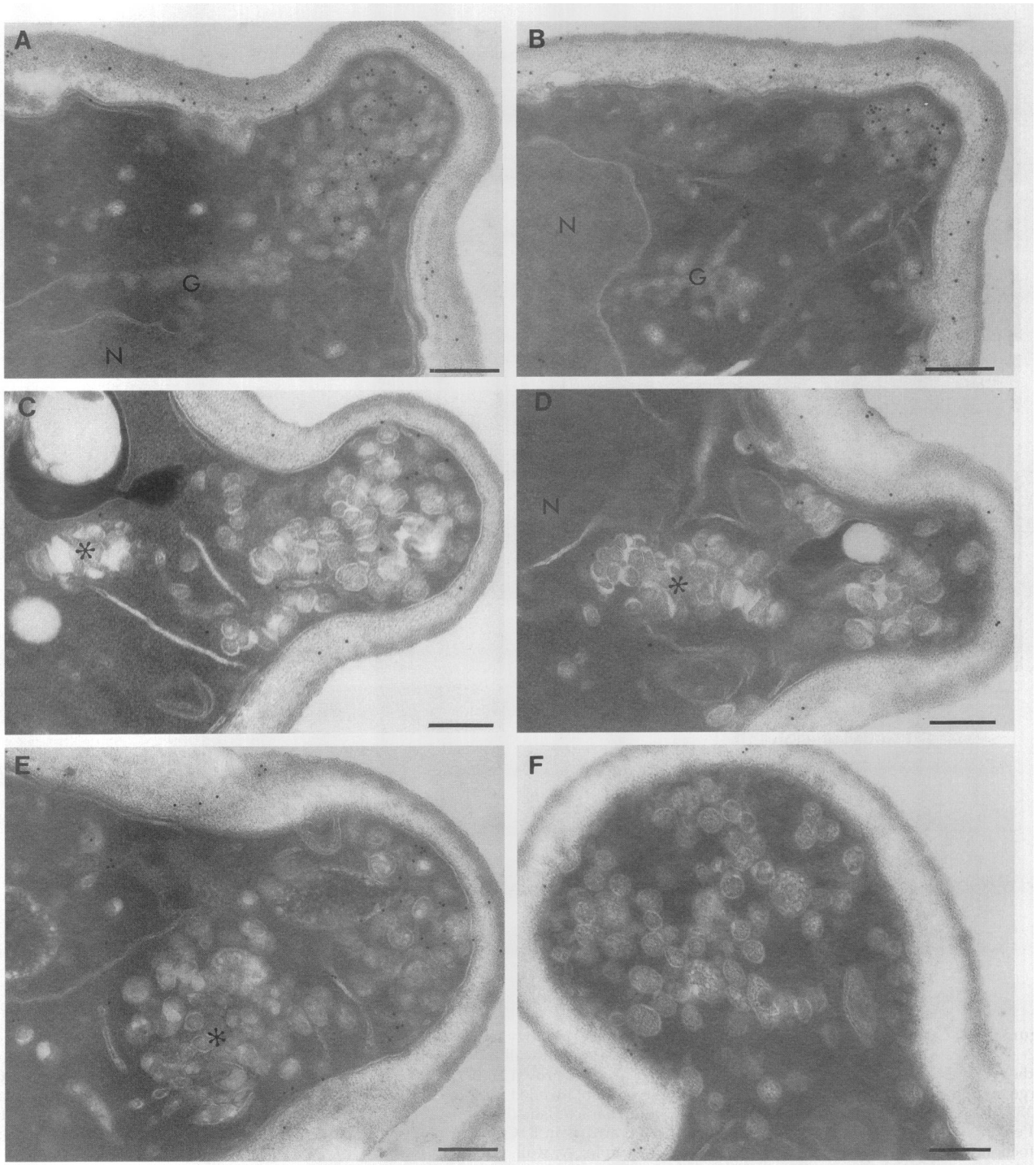

Figure 2. Vesicles that accumulate in *sla2* mutants do not react with anti-Sec4p antibodies. (A and B) Wild-type (RH448) small budded cells labeled with anti-Sec4p antibody that stains large, 40- to 60-nm, vesicles that fill the small buds. Note the position of Golgi membranes at the base of the neck of the small buds. (C–F) *sla2–41* cells (RH1597) grown at 37°C for 1.5 h. Note very sparse Sec4p localization to the large vesicles nearer the bud tips and absence Sec4p localization to the accumulated clustered vesicles (*) positioned at the base of the neck of the three small buds shown in C–E. Symbols are as in Figure 1. Bars, 0.25 μm.

bud early in the yeast cell cycle. In the *sla2* mutants, we consistently observed clusters of vesicles at the base of the neck of early buds (see Figure 2, C–E, for examples) as well as at the tip of larger buds. Thus, it seemed possible that the vesicles accumulated in the *sla2* mutants might represent aberrant Golgi membranes or pos-

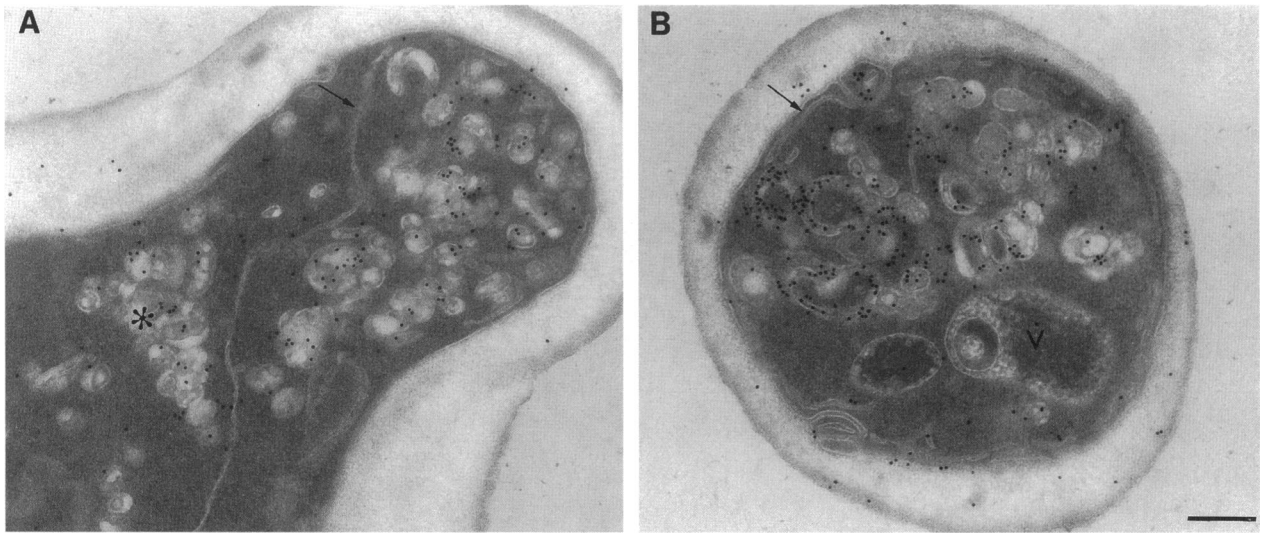

Figure 3. Vesicles that accumulate in *sla2* mutants are reactive with antibodies directed against α-1,6-mannose modifications. *sla2* mutants were incubated at 37°C for 1.5 h. (A) An *sla2–41* (RH1597) cell; note vesicles within the bud and a cluster of vesicles at the bud neck. (B) An *sla2Δ1* (DBY5908) cell containing ring-like membrane structures. Note the absence of localization to the ER membranes (arrows). Bars, 0.25 μm.

sibly Golgi-derived transport vesicles. In yeast, outer chain glycosylation of secreted proteins is initiated in an early (*cis*-Golgi) compartment with the addition of α-1,6-mannose residues (Esmon *et al.*, 1981; Ballou, 1982; Franzusoff and Schekman, 1989; Graham and Emr, 1991). Therefore, α-1,6-mannose modification can be used as a marker for secreted proteins that have passed through this Golgi compartment (Preuss *et al.*, 1992).

To see whether the vesicles that accumulated in the *sla2* cells contained α-1,6-mannose-modified cargo and were thus Golgi-derived, we conducted immuno-EM experiments using antiserum directed against α-1,6-mannose (Figure 3). When examined by immuno-EM, most of the large, 40- to 60-nm, vesicles that accumulated in *sla2* mutants displayed some localization of the antiserum directed against α-1,6-mannose. The clusters of vesicles (Figure 3A) and the ring-like membrane structures that were occasionally observed (10% of cell sections) in the *sla2* deletion strains at nonpermissive temperature labeled consistently and often heavily with the anti-α-1,6-mannose antiserum (Figure 3B). No anti-α-1,6-mannose labeling was observed on the nuclear or peripheral ER in either mutant or wild-type cell sections. These results suggest that the vesicles that accumulate in these mutants are, in fact, Golgi-derived.

Ypt1p, like Sec4p, is a small GTPase; the sequences of the two proteins are highly homologous and their function is largely preserved in chimeras made between them (Schmitt *et al.*, 1986; Segev and Botstein, 1987; Schmitt *et al.*, 1988; Segev *et al.*, 1988; Dunn *et al.*, 1993). However, unlike Sec4p, Ypt1p is required for vesicular transport early in the secretory pathway, between the ER and the Golgi (Segev *et al.*, 1988; Bacon *et al.*, 1989). More recently, Ypt1p has been shown to be required for intra-Golgi protein transport (Jedd *et al.*, 1995). Previously we had shown that Ypt1p is associated with membrane compartments to which known yeast Golgi proteins also are located (Pruess *et al.*, 1992). Therefore, to determine whether the vesicles in the *sla2* mutants were accumulating at a Ypt1p-associated transport step, we conducted immuno-EM experiments using affinity-purified antibodies directed against Ypt1p.

Anti-Ypt1p antibodies applied to *sla2* cell sections, taken from samples grown either at 25°C or incubated at 37°C, did indeed label the large, 40- to 60-nm, vesicles that accumulated within medium- and large-sized buds (Figure 4). Labeling for Ypt1p was strongest on the vesicles clustered at the base of the neck of small buds as well as clusters located within larger sized buds (Figure 4, A, C, and E). Importantly, there was no localization of the anti-Ypt1p antibodies to the 40- to 60-nm vesicles that filled the early small bud that, it will be recalled, labeled abundantly on wild-type cells sections, with antibodies to Sec4p (see Figure 2, A and B; Figure 4C). Additionally, Ypt1p antibodies also stained vesicles associated with the ring-like membrane structures (Figure 4F) observed in the deletion strains incubated at 37°C. Notably, anti-Ypt1p antibodies applied to wild-type cell sections localized 40- to 60-nm vesicles that often appeared to be clustered (Figure 5, A and B). However, these

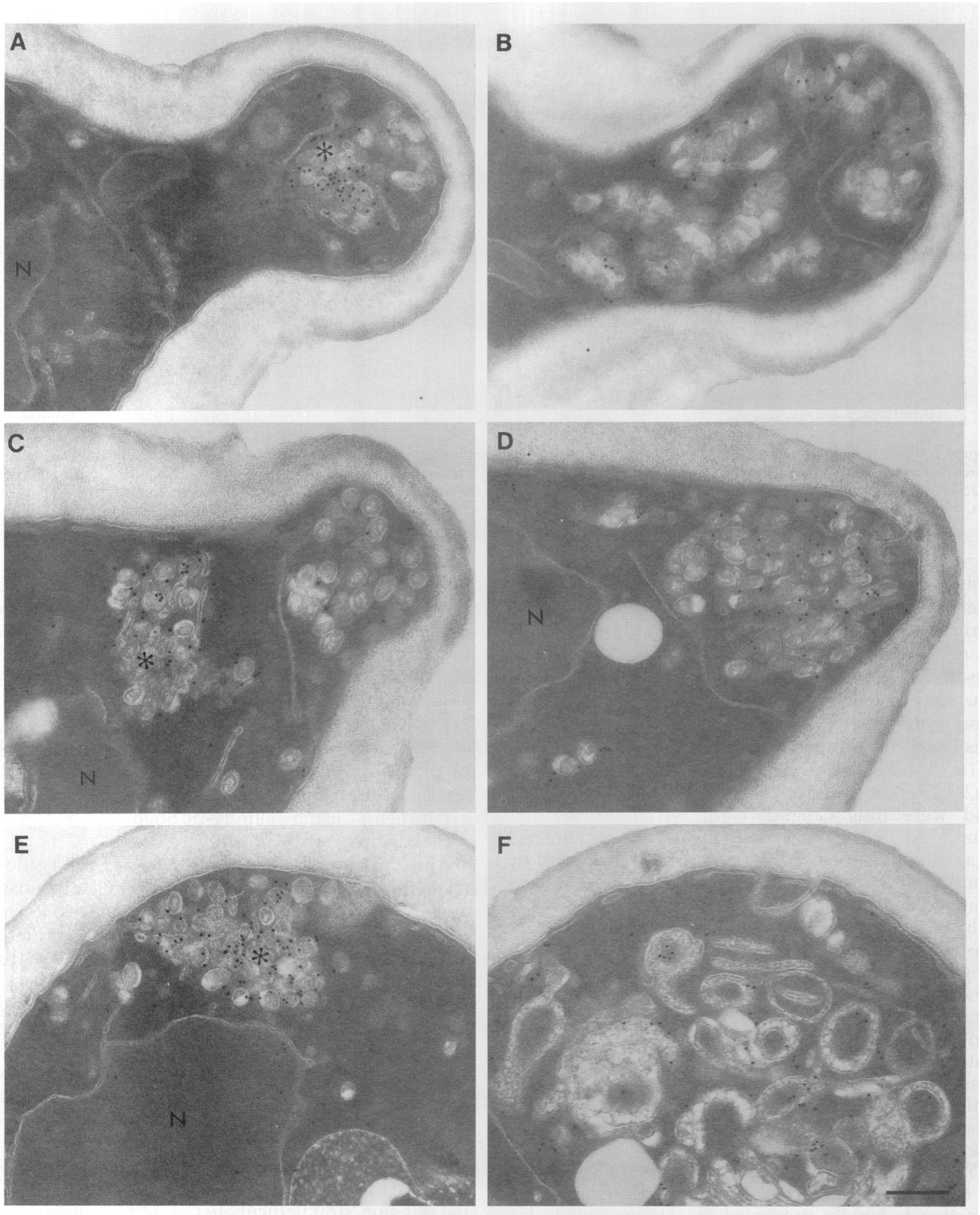

Figure 4. Anti-Ypt1p antibodies strongly label vesicles accumulated in *sla2* cells grown at 25°C (A and B) and incubated at 37°C (C–F). Shown is antibody localization to vesicles clustered (*) at the base of the bud and at the bud tip (A, C, and E) as well as to vesicles dispersed within the bud (B and D) of *sla2–41* (RH1597) cells incubated at 37°C for 1.5 h. (F) Ypt1p localization to vesicles associated with the ring-like membrane structures observed in *sla2*Δ cells (RH3212 shown). Bar, 0.25 μm.

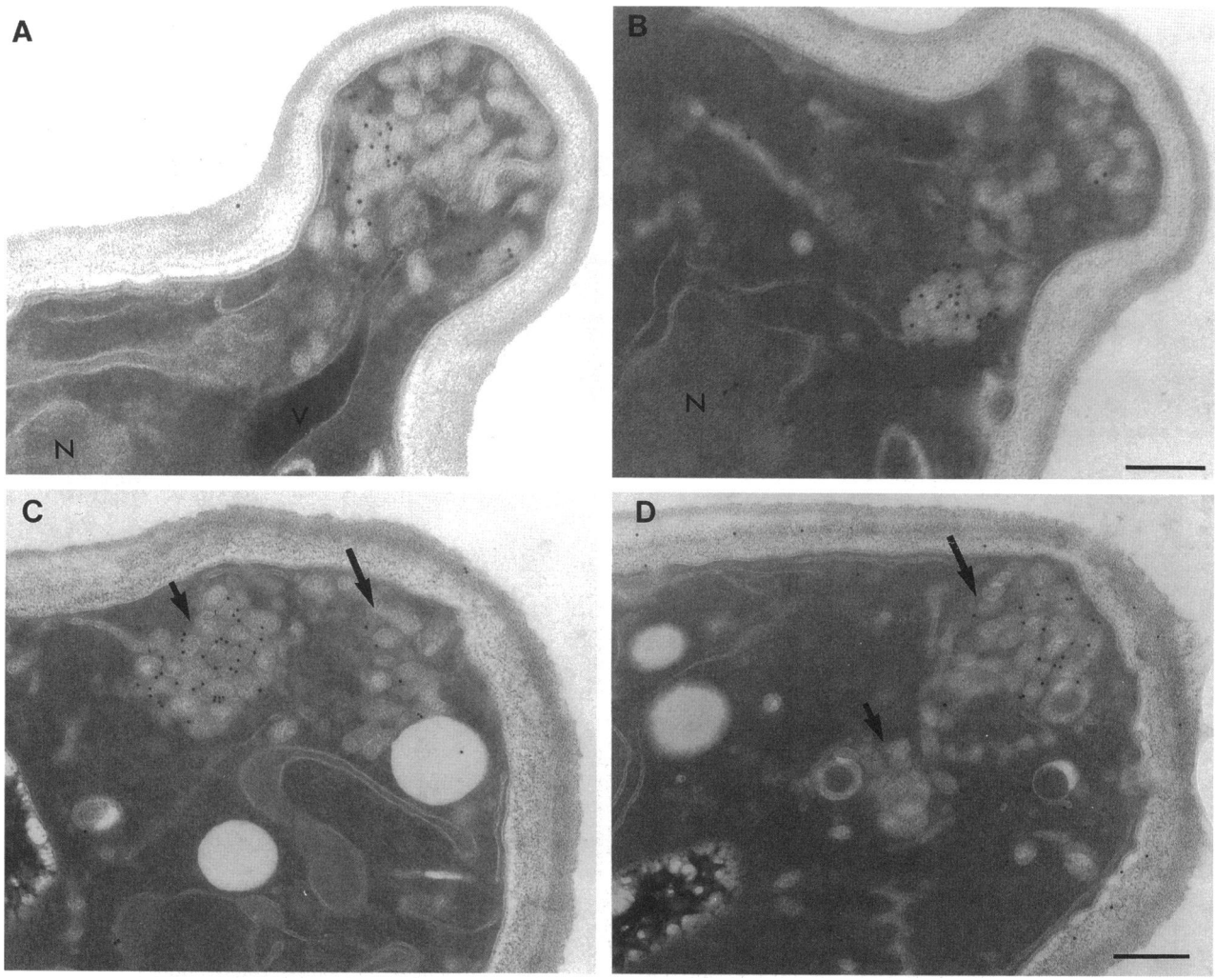

Figure 5. Vesicle clusters labeling with anti-Ypt1 antibody in buds under various conditions. (A and B) Immunolocalization of anti-Ypt1p antibodies to WT (RH448) cell sections. (C and D) α-Factor-arrested *sla2–41* (RH1597) cells incubated at 37°C for 1 h and immunolocalized with antibodies directed against Ypt1p (C) and against Sec4p (D); note differential labeling according to position of vesicles in the cell. Short arrows point to large vesicles clustered at the base of the shmoo; long arrows point to vesicles accumulated at shmoo tip. Bars, 0.25 μm.

Ypt1p positive vesicles were observed infrequently and generally only within medium sized buds.

α-Factor Arrested sla2–41 Cells Accumulate Sec4p- and Ypt1p-Containing Vesicles

Exposure to the yeast mating pheromone, α-factor, causes yeast cells of the **a**-mating type (Mat**a**) to arrest in G_1 and, in preparation for mating, to differentiate into pear-shaped cell (shmooing; reviewed in Cross *et al.*, 1988). The apex of this cell is called the shmoo tip and many components of the yeast cell become polarized toward the shmoo tip in a manner similar to that observed in small budded cells (for recent reviews, see Chant, 1996; Drubin and Nelson, 1996). Polarization of secretory components, particularly Golgi membranes and late secretory vesicles, in α-factor-exposed G_1-arrested cells and in non-α-factor-exposed small budded cells appears to be analogous (Baba *et al.*, 1989; Preuss *et al.*, 1992). The vesicles that accumulate at the shmoo tip, like those that accumulate in the small bud, were therefore presumed to be Sec4p-containing vesicles. Thus, by exposing Mat**a** cells to α-factor, it is possible to obtain a large population of cells that mimic the small budded stage of the cell cycle. We used this technique to investigate the characteristic positioning of clustered Ypt1p-positive vesicles at the base of the neck of small budded *sla2* cells and to see if Sec4p-positive vesicles appear near the shmoo tip.

sla2–41 cells were concurrently exposed to α-factor (2.5 μM) and shifted to 37°C for 1 h and then prepared

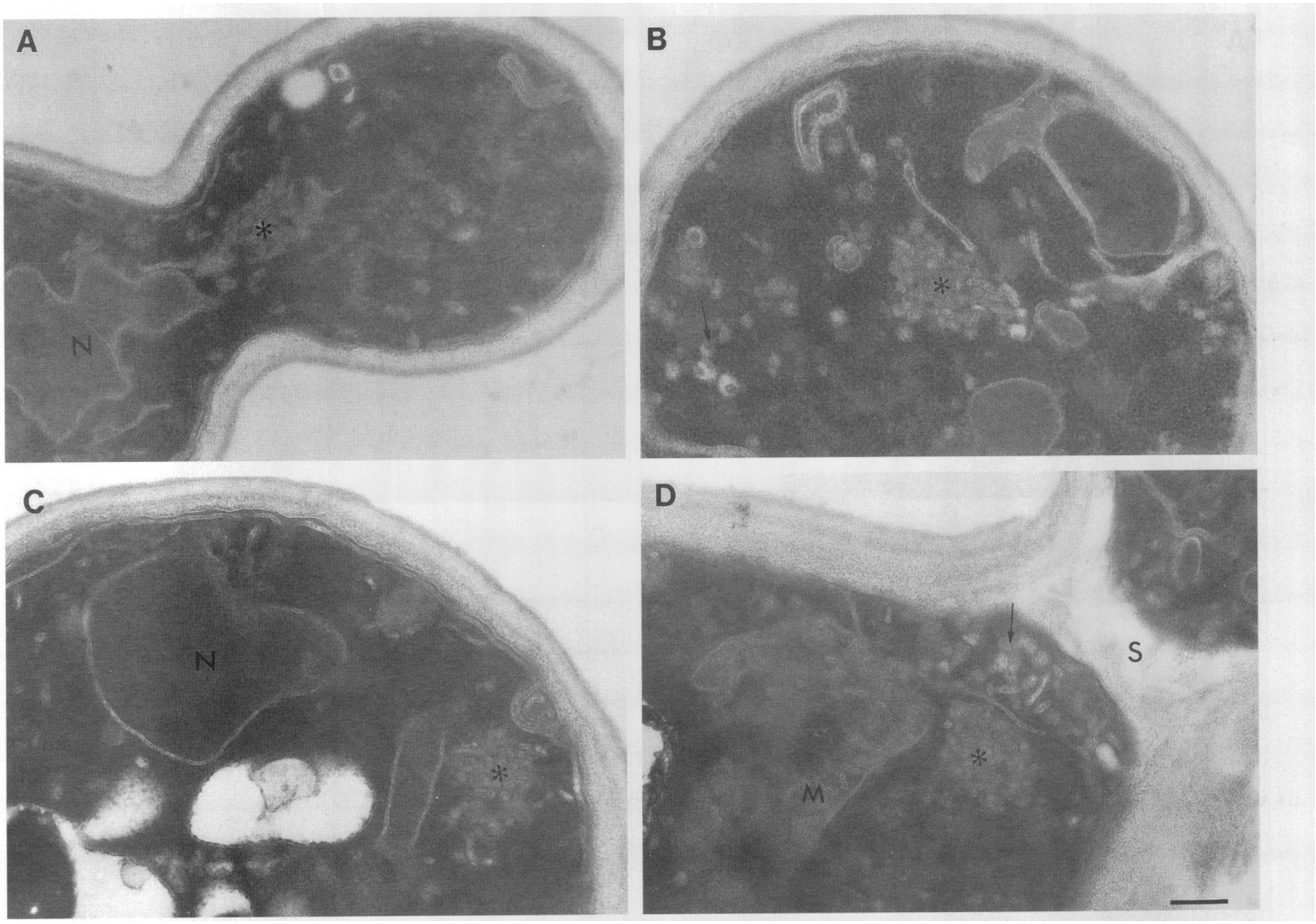

Figure 6. Vesicle accumulation in *sla2* mutants requires an intact early secretory pathway. (A and B) Cell sections of a *sec17–1* (DBY6538) single mutant incubated at 37°C for 1 h; note numerous small (20–30 nm) vesicles that often form aggregates (*) and absence of cell wall defects. (C and D) Cell sections of *sec17–1 sla2–5* double mutant (DBY6540) cells incubated for 1 h at 37°C. Note small vesicles, often aggregated together, along with occasional large, 40- to 60-nm, vesicles (long arrows). Note also characteristic cell wall defect in mothers. Bar, 0.25 μm.

for immuno-EM. Shmooed *sla2–41* cells revealed a consistent positioning of a cluster of large vesicles at the base of the shmoo tip and an accumulation of similarly sized vesicles within the shmoo tip. We observed strong localization of the anti-Ypt1p antibodies to the clustered vesicles located at the base of the shmoo (Figure 5C) and no localization to the vesicles located at the shmoo tip. In contrast, the vesicles located at the shmoo tip were immunoreactive with anti-Sec4p antibodies, but the clustered vesicles were not (Figure 5D).

These results suggest strongly that the location of clustered, Ypt1p-containing vesicles at the base of the neck of small budded *sla2* cells is a spatially and temporally specific event analogous to the positioning of the wild-type Golgi compartment at the base of the neck of small budded cells. Most importantly, the localization of anti-Sec4p antibodies to the vesicles accumulated at the shmoo tip shows that in the *sla2* mutants Sec4p-containing vesicles are indeed present and can be made to accumulate, as in wild-type cells, in an α-factor-dependent manner.

Secretory Defects in Two Early sec Mutants sec12–4 and sec17–1 are Epistatic to Those of sla2–5

To confirm that the vesicles that accumulate in the *sla2* mutants were not aberrant ER membranes or aberrant ER-to-Golgi vesicles, we examined double mutants. The secretory mutant *sec12–4* at its nonpermissive temperature abolishes protein export from the ER and accumulates ER membranes (Novick *et al.*, 1980; Kaiser and Schekman, 1990). The *sec17–1* secretory mutant disrupts ER-to-Golgi transport and accumulates small, 20- to 30-nm (using our methods), vesicles (Figure 6, A and B; see Novick *et al.*, 1980; Kaiser and Schekman, 1990). Double-mutant haploid strains containing the *sla2–5* allele in pair-wise combination with the *sec12–4* and *sec17–1* secretion mutants were con-

structed and confirmed by using complementation analysis (see MATERIALS AND METHODS).

Double mutants grown at 25°C contained large, 40- to 60-nm, vesicles and were morphologically similar to the *sla2* mutants grown at 25°C. However, when incubated at 37°C the double mutants accumulated secretory structures characteristic of the secretory mutant's defect. The *sla2–5 sec12–4* double mutants, at 37°C, accumulated ER membranes and the *sla2–5 sec17–1* double mutants accumulated small, 20- to 30-nm, vesicles; the latter are shown in Figure 6, C and D. These results demonstrate that vesicle accumulation in the *sla2* mutants is dependent upon the *SEC17*-mediated ER-to-Golgi transport step of the secretory pathway.

It should be noted that the double wall phenotype of the *sla2* mutants was observed in the *sec12–4 sla2–5* and the *sec17–1 sla2–5* double mutants grown at 25°C or incubated at 37°C but not in the *sec* mutants alone (compare Figure 6, A and B to C and D).

sla2 Mutants Are Partially Defective in the Secretion of Hyperglycosylated Invertase

The accumulation of large vesicles in the *sla2* mutants suggested a possible defect in protein secretion similar to that observed in actin mutants. Previous biochemical analysis of the *act1–1* allele demonstrated defects in the secretion of fully glycosylated invertase, suggesting a partial block in Golgi-to-plasma membrane transport (Novick and Botstein, 1985). However, localization of Ypt1p antibodies to the vesicles that accumulate in the *sla2* actin cytoskeleton mutants suggested to us a defect in intra-Golgi transport. To test this and to determine more specifically where in the secretory pathway *sla2* mutants are defective, we undertook a biochemical analysis of protein secretion in the *sla2* mutants. To assess protein traffic through different stages of the secretory pathway, we followed the transport and maturation of three different marker proteins, carboxypeptidase Y (CPY), a glycophospholipid-anchored surface protein (Gas1p), and invertase. Each of these proteins undergoes compartment-specific N-linked glycosylation modification and/or proteolytic processing, and each can be exploited to measure transport rates through different stages of the secretory pathway (Schimmoller *et al.*, 1995).

We first investigated the integrity of the vacuole biogenesis pathway, which uses the ER and Golgi portions of the secretory pathway, by following the maturation of CPY. Upon arrival at and subsequent transport through the Golgi compartment, the ER precursor p1CPY is converted to the fully glycosylated protein p2CPY, which is then transported from a late Golgi compartment to the vacuole. Arrival of p2CPY in the vacuole is accompanied by proteolytic processing of the protein to its fully active mature form, mCPY. Cultures of wild-type (*SLA2*) and two kinds of

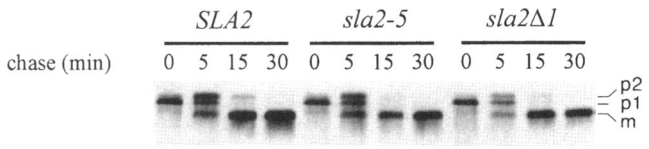

Figure 7. CPY maturation occurs with wild-type kinetics in both *sla2–5* and *sla2Δ1* mutants. Cells were grown 24°C and metabolically labeled at 37°C after a 15-min preincubation. CPY was immunoprecipitated from total cell lysates at the indicated times. Both the conversion of p1CPY to p2CPY and the conversion of p2CPY to mCPY occurs with wild-type kinetics in *sla2* mutants. p1CPY, ER core-glycosylated form of CPY; p2CPY, Golgi-modified form of CPY; m, mature form of CPY.

mutants (*sla2–5* and *sla2Δ1*) were grown at 24°C, and shifted to 37°C for 15 min prior to initiating a pulse-chase experiment. Cells were harvested at 0, 5, 15, and 30 min after the pulse and CPY was immunoprecipitated from total cell lysates. As shown in Figure 7, CPY matures with wild-type kinetics in both sla2–5 and *sla2Δ1* mutants. This result indicates that protein traffic from the ER to the Golgi as well as through the late Golgi compartment to the vacuole is normal in the absence of *SLA2* function.

Because transport from the ER to the Golgi compartment is differentially regulated for some cargo molecules (Schimmoller *et al.*, 1995), we also followed the maturation kinetics of the GPI-anchored protein Gas1p. Gas1p undergoes N-linked core glycosylation in the ER and outer-chain glycosylation upon arrival in the Golgi compartment. Wild-type and mutant (*sla2Δ2*) cells were grown at 24°C and incubated at 24°C or 37°C for 15 min prior to initiating a pulse-chase experiment. Cells were harvested at different time points between 0 and 60 min after an initial 4-min pulse and then Gas1p was immunoprecipitated from total cell lysates. As shown in Figure 8, Gas1p acquired Golgi-specific modifications in the *sla2* deletion mutant with kinetics identical to that observed in wild-type cells. This is further evidence that transport from the ER to the Golgi apparatus is not impaired in the absence of *SLA2* function.

The soluble periplasmic enzyme invertase was used to assess protein transport from the Golgi compartment to the plasma membrane. Upon transport from the ER to the Golgi compartment, invertase is converted from its core-glycosylated form to a hyperglycosylated Golgi form, which is subsequently secreted into the periplasmic space. Wild-type (*SLA2*) and mutant (*sla2–5*, *sla2Δ1*) cells were grown at 24°C, converted to spheroplasts, and then shifted to low-glucose medium to induce invertase expression. Before initiating the pulse-chase protocol, cells were preincubated for 15 min either at 24°C or 37°C. After a 4-min pulse, cells were harvested at 0, 5, 15, and 30 min and centrifuged to separate internal (nonsecreted) from external (secreted) invertase. Invertase from these two

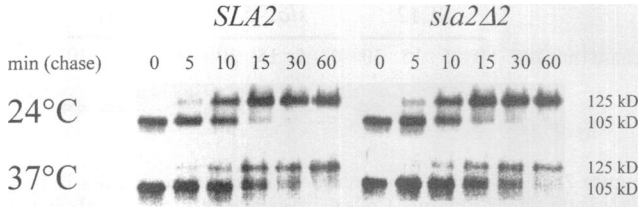

Figure 8. Gas1p matures with wild-type kinetics in *sla2Δ2* mutants. Cells were grown at 24°C, shifted for 15 min to 24°C and 37°C, respectively, before a pulse-chase regimen was performed. Gas1p was recovered from total cell lysates by immunoprecipitation. Maturation of Gas1p at 24°C and 37°C, respectively, occurs with wild-type kinetics independent of an intact *SLA2* gene. 105 kD, ER core-glycosylated Gas1p; 125 kD, Golgi-modified mature form of Gas1p.

fractions was then recovered by immunoprecipitation. As can be seen in Figure 9, there is a minimal defect in invertase secretion in the *sla2* mutants at their permissive growth temperature. In contrast, at 37°C, a significant amount of invertase accumulated inside the *sla2–5* and *sla2Δ1* mutants. Significantly, this internal invertase is hyperglycosylated, consistent with the previous observations indicating that intra-Golgi transport is not perturbed in the *sla2* mutants. Independent experiments showed that the secretion defect exhibited by the *sla2* mutants is not due to differences in the extent of sheroplast formation at 24°C and at 37°C (Wesp and Riezman, unpublished observations).

Taken together these results suggest that the *sla2* mutants, as previously shown for the *act1–1* mutant, are partially defective in the late Golgi-to-plasma membrane steps of protein secretion.

Immuno-EM Characterization of an Actin Mutant, act1–1

As we have shown, *sla2* mutants accumulate vesicles and exhibit secretory defects similar to those previously observed in actin mutants. We therefore wished to confirm that the *sla2* mutants were accumulating the same class of secretory vesicles that accumulates in the actin mutants. To this end, we conducted immuno-EM experiments on the *act1–1* mutant using

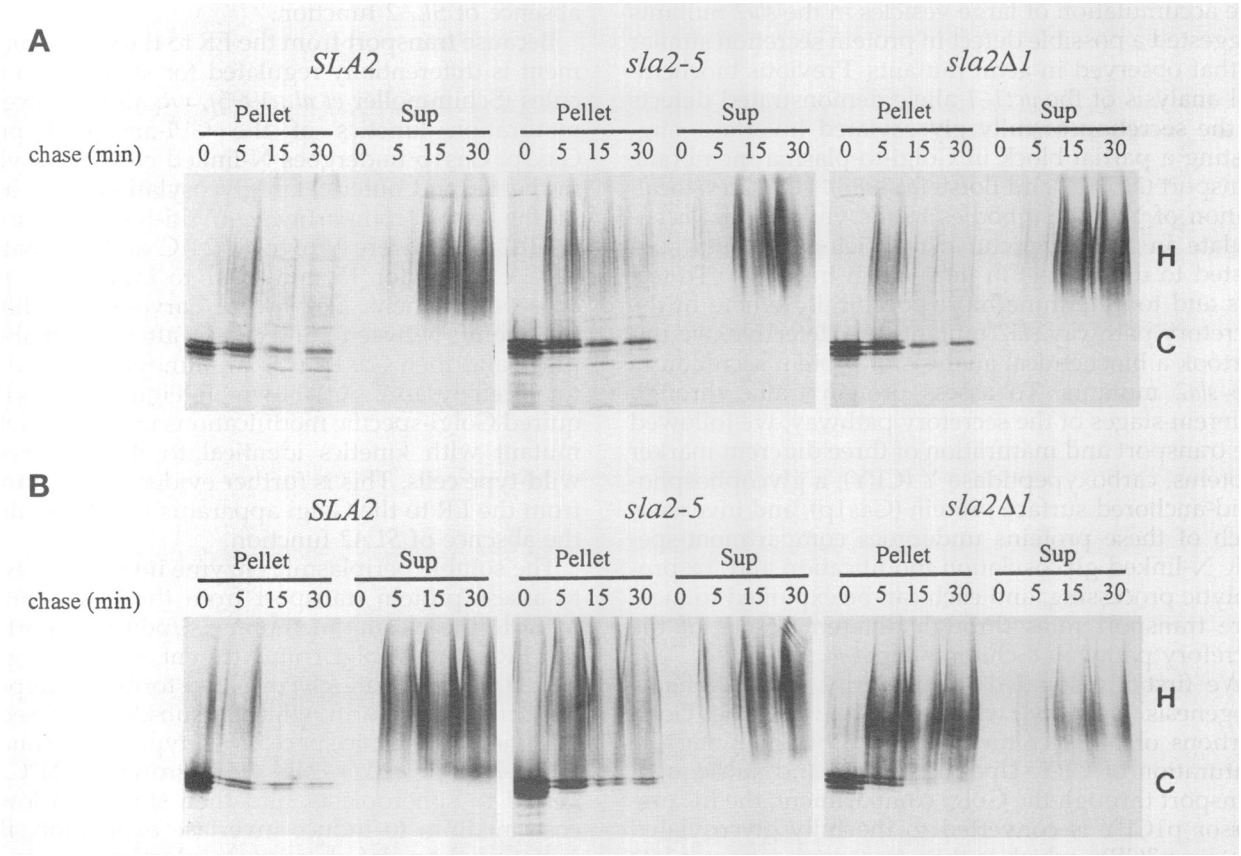

Figure 9. *sla2* mutants show an invertase secretion defect at 37°C. Cells were grown at 24°C, converted to spheroplasts, and resuspended in low glucose medium to induce invertase expression. After a 15-min preincubation at either 24°C (A) or 37°C (B), a pulse-chase protocol was performed. At the times indicated, cells were harvested and pelletted to separate secreted (Sup) from internal (Pellet) proteins. Invertase was recovered from both fractions by immunoprecipitation. C, ER core-glycosylated invertase; H, Golgi-modified hyperglycosylated invertase.

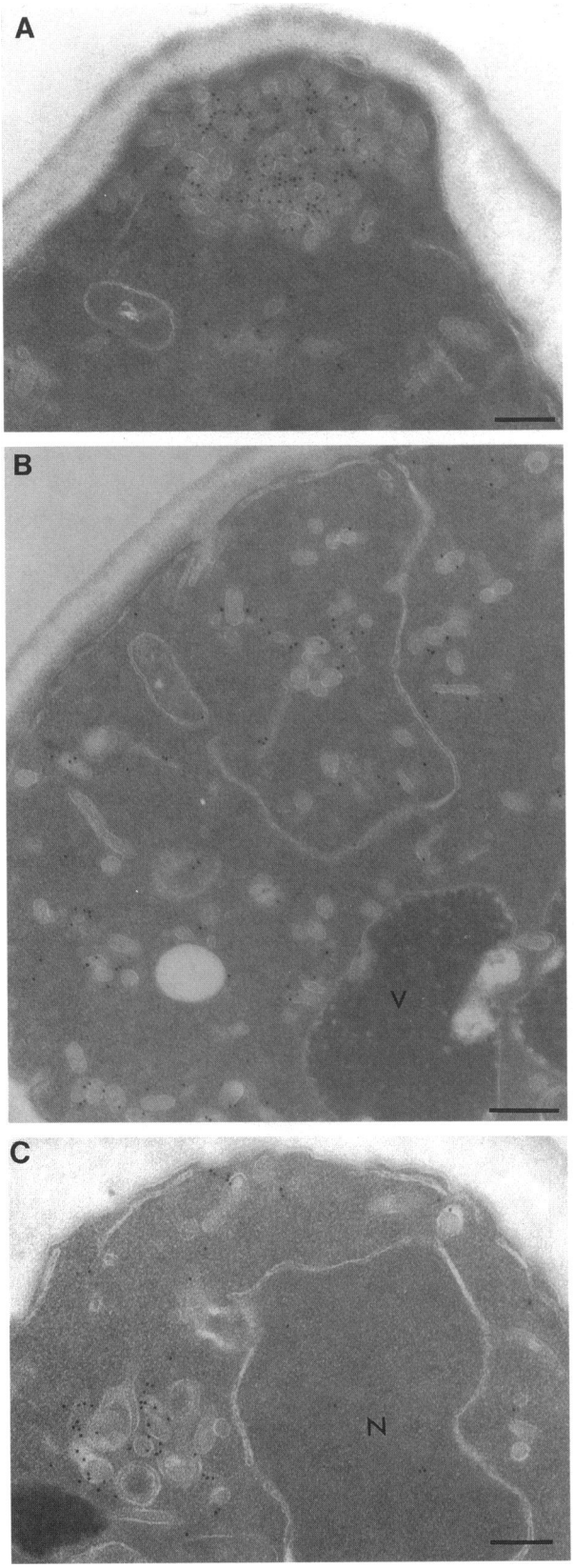

affinity-purified antibodies directed against Ypt1p and Sec4p.

Like the *sla2* mutants, *act1–1* exhibited a polarized accumulation of large, 40- to 60-nm, vesicles at 25°C and at 37°C. However, in contrast to the *sla2* mutants, vesicle accumulation in the *act1–1*, after 1 h at 37°C, was not as strongly polarized into the bud. Figure 10 shows that the vesicles that accumulated in the actin mutant did indeed label with antibodies directed against Ypt1p. Like the *sla2* mutants, aggregates of vesicles located at the early bud neck of *act1–1* cells labeled with the anti-Ypt1p antibodies (Figure 10A), whereas vesicles located within the early bud did not. At 37°C the *act1–1* mutant also formed ring-like membrane structures (Figure 10C) similar to those occasionally observed in the *sla2* deletion mutants incubated at 37°C (see above Figure 4F). As in the *sla2* mutants, the vesicles associated with these ring-like membrane structures labeled with antibodies directed against Ypt1p.

Vesicles located within the small bud as well as at the septum and bud tips showed little labeling with anti-Sec4p antibodies. The level of anti-Sec4p labeling of secretory vesicles located at areas of cell growth was consistent with that observed in the *sla2* mutants and, as in the *sla2* mutants, was sparse relative to the anti-Sec4p labeling observed in wild-type cell sections (our unpublished observations).

These results indicate that the actin cytoskeleton mutants *sla2* and *act1–1* have analogous defects in cell surface growth and accumulate similar secretory vesicles.

The Late Secretory Mutants sec1–1, sec6–4, and sec4–8 Accumulate Ypt1p- and Sec4p-containing Vesicles

Our biochemical results of *sla2* mutants, together with the cell cycle-dependent localization of clustered vesicles at the base of the neck of small budded cells, strongly suggest a secretory defect either in a late Golgi compartment or in Golgi-to-plasma membrane transport. However, the immunolocalization of Ypt1p to vesicles that accumulate in both the *sla2* and the *act1–1* mutant would seem to indicate a defect in intra-Golgi transport. It is possible to postulate that Ypt1p, besides acting in ER-to-Golgi and early intra-Golgi transport, is associated with later steps in the secretory pathway. If Ypt1p were in fact associated with a late step in the secretory pathway, some of the

Figure 10. *act1–1* cells accumulate the same type of vesicles as does *sla2* mutant cells. Immunolocalization of antibodies directed against Ypt1p to *act1–1* (DBY1691) cells incubated at 37°C for 1 h. (A) Note localization to vesicles clustered at the neck of the bud. (B) Note localization to vesicles dispersed within the mother and bud cytoplasm. (C) An example of the occasional ring-like membrane structures; note localization. Bar, 0.25 μm.

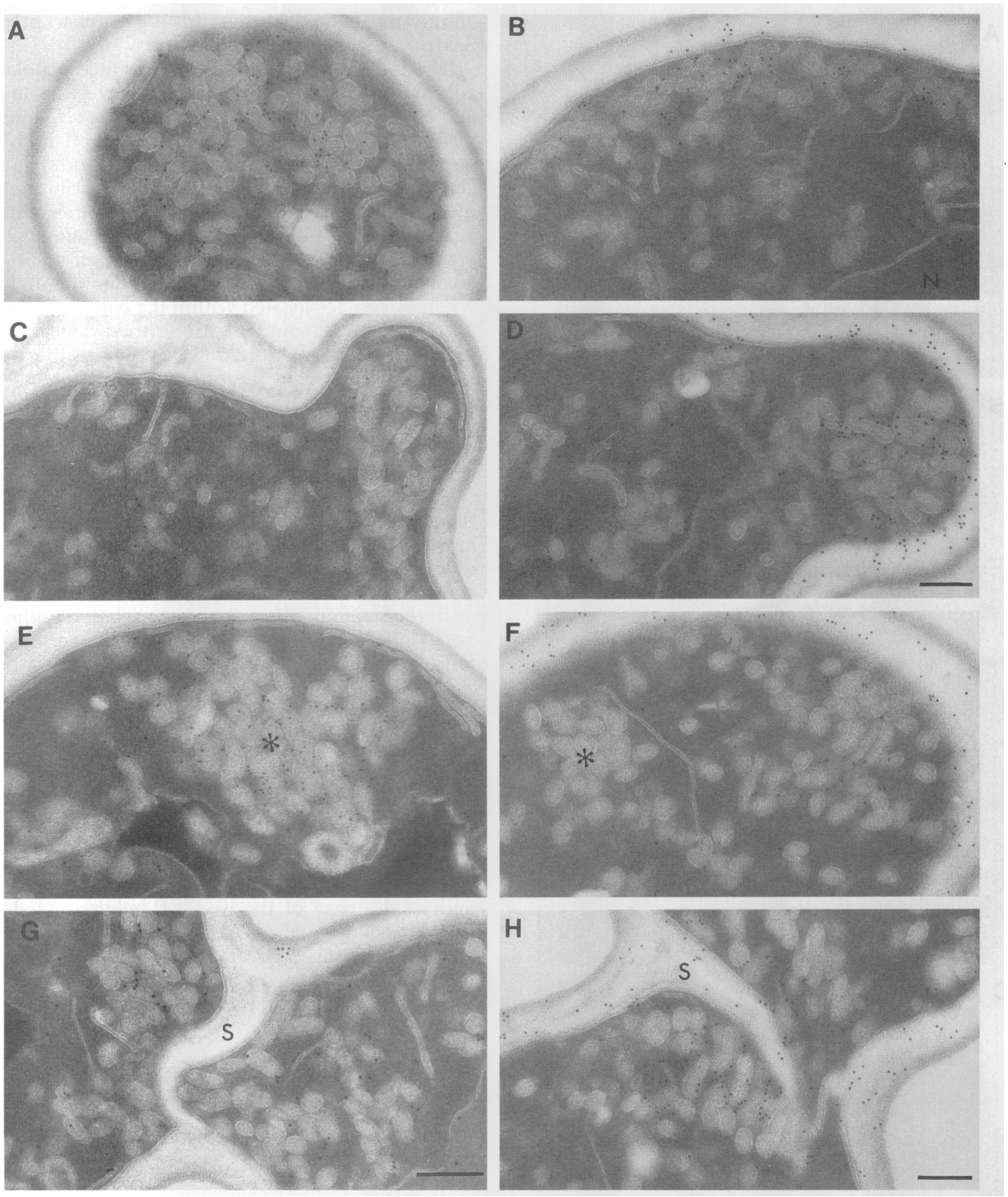

Figure 11. *sec1–1* and *sec6–4* mutants accumulate vesicles that label for Ypt1p as well as Sec4p. (A–D) *sec1–1* (DBY5888) incubated at 37°C for 1 h. Immunolocalization of antibodies directed against Ypt1p (A and C) and against Sec4p (B and D) is shown. Note in small buds (C and D), vesicles label with anti-Sec4p antibodies and not Ypt1p antibodies. (E–H) *sec6–4* (DBY5889) incubated at 37°C for 1 h. Immunolocalization of antibodies directed against Ypt1p (E and G) and against Sec4p (F and H) is shown. *, Clustered vesicles that label with anti-Ypt1p antibodies (E) and not anti-Sec4p antibodies (F). Bars: A–D, 0.25 μm; E and G, 0.25 μm; F and H, 0.25 μm.

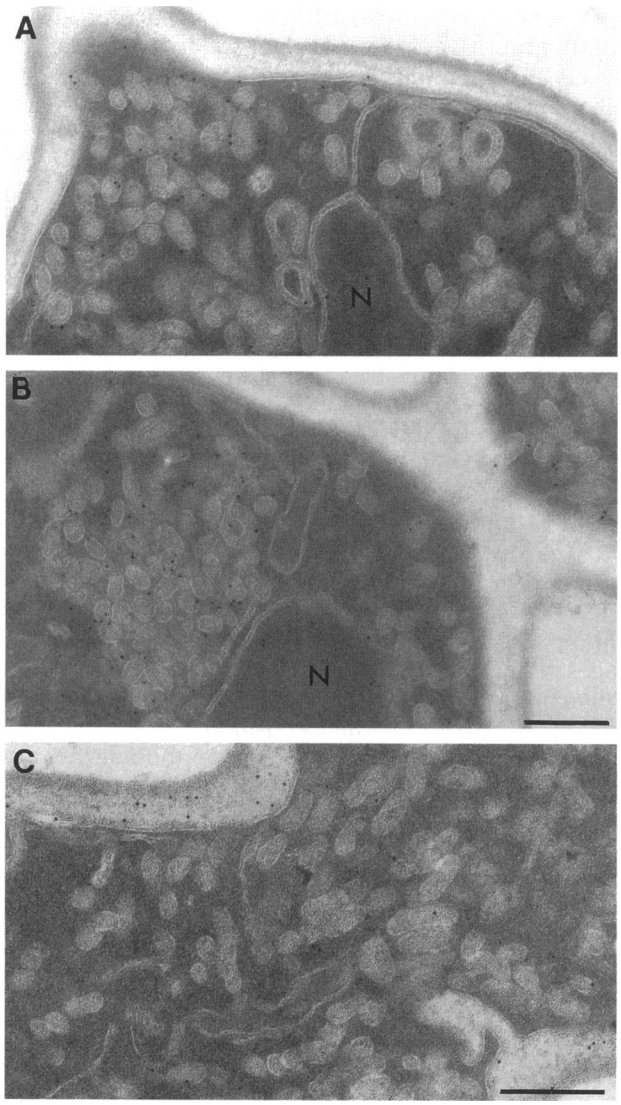

Figure 12. *sec4–8* mutants accumulate Ypt1p containing vesicles. Immunolocalization of antibodies directed against Ypt1p (A and B) and against Sec4p (C) to *sec4–8* (DBY5894) cells incubated at 37°C for 1 h. Note in C that the anti-Sec4p antibodies do not localize to late secretory vesicles in the *sec4–8* cells incubated at 37°C because antibody has a greatly reduced affinity for the mutant protein (Goud *et al.*, 1988). However, anti-Sec4p antibodies nevertheless label the cell wall of *sec4–8* cells incubated at 37°C, indicating that the cross-reacting antigen is unlikely to be Sec4p.

known late-acting secretory mutants might be expected to accumulate secretory vesicles that label with antibodies directed against Ypt1p. To test this, we examined three well-characterized late secretory mutants, *sec1–1*, *sec6–4*, and *sec4–8* (Novick *et al.*, 1980, 1981; Govindan *et al.*, 1995).

Consistent with previous reports, *sec1–1*, *sec6–4*, and *sec4–8* cells incubated at their nonpermissive temperature (37°C) for 1 h accumulated numerous large secretory vesicles, and this accumulation was polarized into the bud (see Figures 11 and 12). Interestingly, the *sec6–4* and *sec4–8* cells incubated at 37°C contained many vesicles that were clustered together in a manner reminiscent of the *sla2* and *act1–1* mutants, suggesting that these mutants accumulate vesicles at a similar step in protein secretion. The *sec1–1* mutant did not show a similar clustering of vesicles. However, it is possible that specific clustering of vesicles does occur in the *sec1–1* mutant but that this clustering is obscured by the dense accumulation of vesicles that is characteristic of this mutant.

Immuno-EM experiments demonstrated that the vesicles that accumulated in *sec1–1*, *sec6–4*, and *sec4–8* were immunoreactive with antibodies directed against Ypt1p (Figure 11, A, C, E, and G; Figure 12, A and B). Further, the clustered vesicles observed in the *sec6–4* and *sec4–8* cells, like those observed in the *sla2* and *act1–1* mutants, were strongly immunoreactive with the anti-Ypt1p antibodies (see Figures 11E and 12C for examples). However, although many vesicles labeled with the anti-Ypt1p antibodies, many vesicles did not label, suggesting that another class of secretory vesicles may be accumulating in these three secretory mutants.

Previous cell fractionation and immunofluorescence light microscopy studies of several vesicle-accumulating late-acting secretory mutants, including *sec1–1* and *sec6–4*, have demonstrated that Sec4p is associated with the vesicles that accumulate in these mutants (Goud *et al.*, 1988). These results prompted us to apply anti-Sec4p antibodies to the *sec1–1* and *sec6–4* cell sections. Not surprisingly, many of the vesicles that accumulated in these two *sec* mutants labeled with antibodies directed against Sec4p (Figure 11). The strongest localization of Sec4p, in both *sec6–4* and *sec1–1*, appeared to be on vesicles accumulated along the plasma membrane, at the septum, at the bud tip, and within the small bud (Figure 11, B, D, F, and H). Further, in the *sec6–4* mutant, as in the *sla2* and the *act1–1* mutants, the anti-Sec4p antibodies did not label the clustered vesicles (for an example see Figure 11F) that, it will be remembered, labeled strongly with anti-Ypt1p antibodies.

The affinity-purified anti-Sec4p antibodies used in our studies have been shown to have a greatly reduced affinity for the mutant sec4–8 protein (Goud *et al.*, 1988). Consistent with that result, we observed no localization of the anti-Sec4p antibodies to the vesicles that accumulated in *sec4–8* cells at 37°C (Figure 12C).

The Organization of the Actin Cytoskeleton Is Disrupted in the Late Secretory Mutant sec4–8

The late *sec* mutants *sec1–1* and *sec6–4* exhibit disorganized actin cytoskeletons when incubated at their

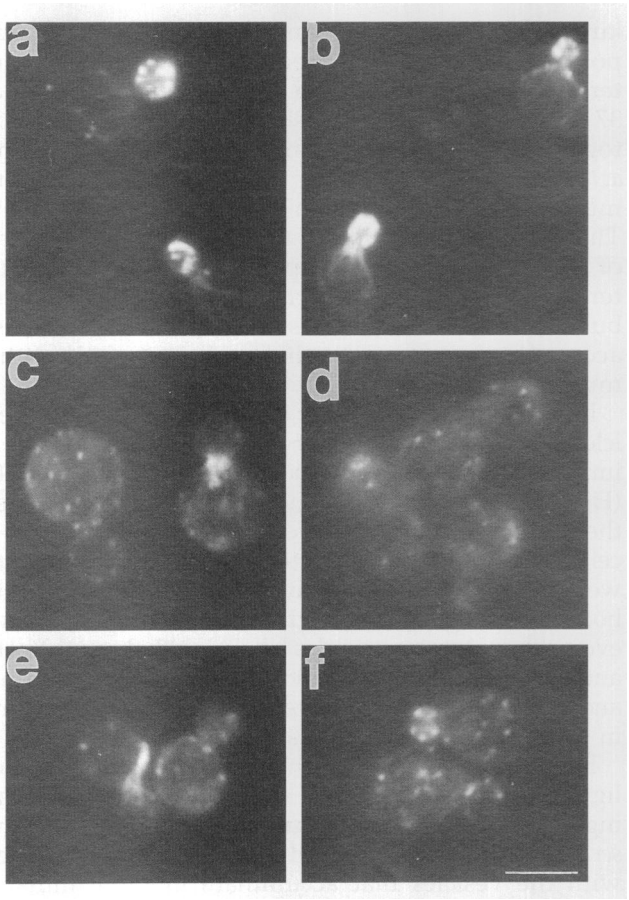

Figure 13. *sec4–8* cells have a depolarized actin cytoskeleton at 36°C. (a and b) Wild-type cells grown at 36°C for 1 h, fixed, and stained with rhodamine-phalloidin. (c–f) Examples of *sec4–8* cells (DBY5894) incubated at 36°C for 1 h. Note that *sec4–8* cells tend to be larger and more round than wild-type cells and contain actin cytoskeletons that are depolarized and generally disorganized. Note also the brightly staining aggregates of actin in the bud neck in c and adjacent to the bud neck in e.

nonpermissive temperature (Lillie and Brown, 1994). This result, along with our observation that the actin cytoskeleton mutants *sla2* and *act1* accumulate Ypt1p-positive vesicles and not Sec4p-positive vesicles, suggests that a defect in the actin cytoskeleton might be the reason for accumulation of Ypt1p positive vesicles in late secretory mutants. To see whether this generalization might extend even to *sec4* mutants, we examined the actin cytoskeleton organization by rhodamine-phalloidin fluorescence microscopy in a *sec4–8* mutant grown at 25°C and incubated at 36°C.

After 30 and 60 min at 36°C, the *sec4–8* mutant cells exhibited obvious defects in the organization of the actin cytoskeleton (Figure 13, c–f). These defects included a depolarized distribution of cortical actin structures, diffuse cytoplasmic staining, loss of brightly stained actin cables, and, occasionally, large brightly staining cortical actin patches. Wild-type controls responded to temperature shift without depolarization of the actin cytoskeleton (Figure 13, a and b). The *sec4–8* actin cytoskeleton defects appear similar to those previously described by Lillie and Brown (1994) for the *sec1–1* and *sec6–4* mutants.

DISCUSSION

The morphological defects commonly observed in mutants defective in the yeast actin genes and in other genes thought to control actin cytoskeleton organization include perturbation of structures associated with secretory pathways. Ultrastructural studies have shown that many actin cytoskeleton mutants specifically accumulate secretory vesicles and membranes. Previous immunofluorescence light microscopy studies of *sla2* mutants revealed the delocalization of cortical actin structures expected of mutations in genes associated with the actin cytoskeleton (Holtzman *et al.*, 1993). In this study we have shown that *sla2* mutants, like *act1* mutants, have defects in cell wall morphology, accumulate large, 40- to 60-nm, secretory vesicles and are defective in the late stages of protein secretion. These phenotypes are entirely consistent with a role for the actin cytoskeleton in protein secretion and wall deposition.

Many, but not all, actin cytoskeleton mutants are also defective in endocytosis (Munn *et al.*, 1995) and *act1* and *sla2(end4)* mutants have been shown to be specifically defective in the internalization steps of receptor mediated endocytosis (Kubler and Riezman, 1993; Raths *et al.*, 1993). However, we do not believe that the secretory defects manifested by the *sla2* and *act1* mutants are an indirect consequence of failure to carry out endocytosis for two reasons. First, *sla2* deletion mutants are completely defective in endocytosis at 24°C but, as we have shown herein, these mutants secrete invertase normally at that temperature. Second, we have observed that wild-type cells do not carry out endocytosis when assayed under conditions suitable to monitor invertase secretion (Wesp and Riezman, unpublished observation). We are thus led to the conclusion that the exocytosis defects observed in these mutants are the direct result of a disorganized actin cytoskeleton.

Actin Cytoskeleton Mutants, sla2 and act1, Accumulate One of the Two Classes of Vesicles that Accumulates in Late Secretory Mutants

Perhaps the most significant finding presented herein is that the *sla2* and *act1–1* mutants specifically accumulate large secretory vesicles to which anti-Ypt1 antibodies localize. In contrast, the late-acting secretion mutants, *sec1–1*, *sec6–4*, and *sec4–8* accumulate similarly large vesicles to which anti-Ypt1p and (with the obvious exception of *sec4–8*) anti-Sec4p antibodies localize. However, it is by no means necessary to believe that there are any vesicles that simultaneously carry

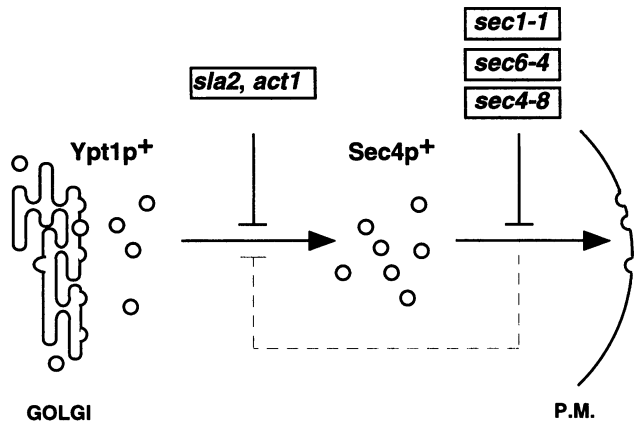

Figure 14. Cartoon illustrates the sequential requirement for actin cytoskeleton function and the late *SEC* gene functions in vesicle trafficking from the late Golgi to the plasma membrane. The actin cytoskeleton is required after the appearance of a Ypt1p-associated vesicle; the late *SEC* genes (*SEC1*, *SEC6*, and *SEC4*) are required at a later step whose failure(s) result in accumulation of Sec4p-associated vesicles. The dashed line connecting the later step to the earlier one indicates the proposed disruption of the actin cytoskeleton secondary to the failure of the later secretion step.

both antigens. Indeed, our aggregate results regarding location and clustering of vesicles in both mutant and wild-type cells suggests that there might be two kinds of vesicles accumulating in these mutants.

In both the late *sec* mutants and the actin cytoskeleton mutants, we observed specific clustering of large secretory vesicles. These clustered vesicles were immunoreactive with antibodies directed against Ypt1p and not with antibodies directed against Sec4p. Also, we demonstrated that the kinetics of protein transport to and through the Golgi apparatus in the *sla2* mutants were similar to that observed in wild-type cells, suggesting that the membrane compartments required for intra-Golgi protein transport are intact. Further, in wild-type cells we could find large Ypt1p-associated vesicles usually in clusters near where Golgi might be. These results suggest that the Ypt1p-associated vesicles are normal compartments and that the different GTPase-containing vesicles constitute two distinct classes, Ypt1p and Sec4p associated.

A straightforward way to interpret these results is to hypothesize that the actin cytoskeleton is functionally involved in a specific step in the latter part of the secretory pathway. A kinetic or absolute defect in this step results in the accumulation of Golgi-derived Ypt1p-associated large vesicles. The hypothesized actin cytoskeleton-dependent step would be prior to the Sec4p-associated vesicle step (Figure 14). A complete consonance with the known facts could be achieved by hypothesizing further that defects in later steps (especially those that result in the accumulation of the classical "late" Sec4p-associated vesicles) result in disorganization of the actin cytoskeleton, which in turn causes a problem at the step in which the cytoskeleton is involved. This idea accounts nicely for the observations that defects in SEC1, SEC6 (Lillie and Brown, 1994), SEC3 (Haarer *et al.*, 1996), and now also SEC4 (Figure 13) result in a similar depolarization of actin staining.

Why Ypt1p should be associated with late secretory vesicles is still unexplained, as previous biochemical and genetic studies have failed to implicate Ypt1p function with vesicle transport from the late Golgi to the plasma membrane. It may be that Ypt1p is associated with these vesicles in a nonfunctional or nonobligatory way. On the other hand, it may be that the Ypt1p-associated vesicles we have identified are intra-Golgi transport vesicles that accumulate due to a more general loss of Golgi compartment organization. Under this hypothesis, the actin cytoskeleton would be implicated in maintenance of the integrity of the Golgi compartment(s) in addition to any role in bringing the Golgi and/or derived vesicles to their proper positions within or near growing membrane surfaces.

This interpretation is somewhat difficult to harmonize with our biochemical analysis of protein transport in the *sla2* mutants. We found that in the *sla2* mutants, CPY, which is transported to the vacuole via a Kex2p-containing late Golgi compartment, is matured with wild-type kinetics. This result would seem to require a functionally intact Golgi in *sla2* mutants. One way to rectify this conflict is to postulate that CPY is transported to the vacuole via a late Golgi compartment that is structurally distinct (and thereby actin independent) from the Golgi compartment(s) utilized for secretion of invertase.

Recently, two distinct classes of late secretory vesicles that carry different protein cargoes have been distinguished on the basis of equilibrium density centrifugation (Harsay and Bretscher, 1995). These vesicles accumulate within and have been purified from extracts of several late-acting secretory mutants, including *sec1–1* and *sec6–4*. This observation has lent credence to the idea that at least two late secretory vesicle types emanate from the yeast Golgi compartment(s) following distinct parallel pathways to the plasma membrane. In that same report, Harsay and Bretscher (1995) also reported an accumulation of secretory vesicles in the *sla2–41(end4–1)* mutant. Importantly, the *sla2–41* vesicles were shown to represent exclusively one of the two vesicles classes shown to accumulate in the late Golgi-to-plasma membrane secretory mutants. We also observed two distinct classes of vesicles accumulated in the late *sec* mutants *sec6–4* and *sec1–1*, only one of which accumulated in the *sla2* mutants we examined. Thus, it may be that the Ypt1p- and Sec4p-associated vesicles we identified constitute the same classes of vesicles identified by Harsay and Bretscher (1995). However, direct correlation of the distinct protein cargoes identified by Harsay and

Bretscher (1995) with the specific GTPase-associated vesicles identified in this study will be necessary to unambiguously confirm any relationship(s) between these vesicle classes.

Roles of the Actin Cytoskeleton in Cell Wall Deposition and Protein Secretion Are Separable

Lastly, we observed defects in cell wall morphology in the *sla2* and *act1* mutants. These cell wall defects could, at least partially, be the result of an endocytosis defect. It has been speculated that endocytosis might be required to maintain a polarized distribution of cell surface proteins, such as cell wall-synthesizing enzymes. Thus, mutants defective in endocytosis would be expected to have a continuous delocalized deposition of cell wall, resulting in the thick multiwalled morphology observed in the *sla2* and *act1–1* mutants. This would be consistent with the constitutive defect in fluid-phase endocytosis observed in *sla2–41* and *act1–1* mutants (Raths *et al.*, 1993; Kubler and Riezman, 1993). However, this interpretation is made less attractive because only a minor defect in the cell wall morphology is observed in a *sac6* deletion mutant (Mulholland and Botstein, personal observation) that has been shown to be totally and constitutively defective in endocytosis (Kubler and Riezman, 1993). Thus, although defects in endocytosis may contribute to delocalized wall deposition, it is most likely not the primary cause.

We have also shown that the defects in cell wall morphology observed in the *sla2* and *act1–1* mutants, unlike their secretory defects, are not temperature sensitive. Furthermore, the *sla2* and the *act1–1* mutants initially accumulate vesicles within the bud (as do the late *sec* mutants) and not in the mother cell where the cell wall defects are observed. Additionally, defects in cell wall morphology were not observed in any of the single *sec* mutants we examined. In contrast, constitutive cell wall defects were observed in the *sec-sla2* double mutants we studied. These *sec-sla2* double mutants showed the temperature-independent mother-cell wall defect of their *sla2* component, and the temperature-dependent secretion defect of their *sec* component—the epistasis was opposite for the two phenotypes. Together these results suggest that the wall defects observed in the actin cytoskeleton mutants do not result trivially from defects in polarized protein secretion.

Rather, our results suggest that the function of the actin cytoskeleton in cell wall deposition and in protein secretion are separable. It has been proposed that the cortical actin patch has a direct role in cell wall biosynthesis (Mulholland *et al.*, 1994). In this report we have shown that the *sla2* and *act1–1* mutants have a constitutive temperature-independent defect in cell wall morphology and it has been previously demonstrated that these mutants have a constitutive temperature-independent delocalization of cortical actin patches (Holtzman *et al.*, 1993). Thus, we speculate that the wall defects observed in these mutants results from the depolarization of the cortical actin cytoskeleton during growth of the mother.

To conclude, our results implicate the actin cytoskeleton in two apparently separable functions. One of these function involves the metabolism of a newly described large post-Golgi secretory vesicle. The other is the previously hypothesized, presumably direct, involvement in cell wall deposition.

ACKNOWLEDGMENTS

We are indebted to Genentech for their generous donation of a Philips EM300 and to Gilbert Keller and Mark Siegel of The Electron Microscopy Facility at Genentech for their continued interest and support. We thank N. Segev for the anti-Ypt1p antibodies, P. Novick for the anti-Sec4p antibodies, A. Franzusoff for the anti-α-1,6-mannose antiserum, and D. Drubin and C. Kaiser for strains. Without their generosity this work would not be easily possible. J.M. also thanks past and present members of the Botstein laboratory for useful discussion. We thank Thomas Aust and Nicolas Stern for technical assistance. Research was supported by grants to D.B. from the National Institutes of Health (GM-46406) and by grants to H.R. from the Canton of Basel-Stadt and the Swiss National Science Foundation.

REFERENCES

Adams, A.E., Botstein D., and Drubin, D. (1989). A yeast actin-binding protein is encoded by *SAC6*, a gene found by suppression of an actin mutation. Science *243*, 231–233.

Adams, A.E.M., Botstein, D., and Drubin, D. (1991). Requirement of yeast fimbrin for actin organization and morphogenesis in vivo. Nature *354*, 404–408.

Adams, A.E.M., and Pringle, J.R. (1984). Relationship of actin and tubulin distribution in wild-type and morphogenetic mutant *Saccharomyces cerevisiae*. J. Cell Biol. *98*, 934–945.

Baba, M., Baba, N., Ohsumi, Y., Kanaya, K., and Osumi, M. (1989). Three-dimensional analysis of morphogenesis induced by mating pheromone a-factor in *Saccharomyces cerevisiae*. J. Cell Sci. *94*, 207–216.

Bacon, R.A., Salminen, A., Ruohola, H., Novick, P., and Ferro-Novick, S. (1989). The GTP-binding protein Ypt1 is required for transport in vitro: the Golgi apparatus is defective in *ypt1* mutants. J. Cell Biol. *109*, 1015–1022.

Ballou, C.E. (1982). Yeast cell wall and cell surface. In: The Molecular Biology of the Yeast *Saccharomyces*, ed. J.N. Strathern, E. Jones, and J. Broach, Cold Spring Harbor, NY: Cold Spring Harbor Laboratory Press, 335–360.

Botstein D., Amberg, D., Huffaker, T., Mulholland, J., Adams, A., Drubin, D., and Streans, T. (1997). The Yeast Cytoskeleton. In: The Molecular and Cellular Biology of the Yeast *Saccharomyces*, ed. J.R. Broach, J.R. Pringle, and E.W. Jones, Cold Spring Harbor, NY: Cold Spring Harbor Laboratory Press.

Chant, J. (1996). Septin scaffolds and cleavage planes in *Saccharomyces*. Cell *84*, 187–90.

Cross, F., Hartwell, L., Jackson, C., and Konopka, J. (1988). Conjugation in *Saccharomyces cerevisiae*. Annu. Rev. Cell Biol. *4*, 429–457.

Drubin, D.G., Miller, K., and Botstein, D. (1988). Yeast actin-binding proteins: evidence for a role in morphogenesis. J. Cell Biol. *107*, 2551–2561.

Drubin, D.G., and Nelson, W.J. (1996). Origins of cell polarity. Cell *84*, 335–344.

Dunn, B., Stearns, T., and Botstein, D. (1993). Specificity domains distinguish the Ras-related GTPases Ypt1 and Sec4. Nature *362*, 563–565.

Esmon, B., Novick, P., and Schekman, R. (1981). Compartmentalized assembly of oligosaccharides on exported glycoproteins in yeast. Cell *25*, 451–460.

Franzusoff, A., and Schekman, R. (1989). Functional compartments of the yeast Golgi apparatus are defined by the *sec7* mutation. EMBO J. *8*, 2695–2702.

Goud, B., Salminen, A., Walworth, N., and Novick, P. (1988). A GTP-binding protein required for secretion rapidly associates with secretory vesicles and the plasma membrane in yeast. Cell *53*, 753–768.

Govindan, B., Bowser, R., and Novick, P. (1995). The role of Myo2, a yeast V myosin, in vesicular transport. J. Cell Biol. *128*, 1055–1068.

Graham, T.R., and Emr, S.D. (1991). Compartmental organization of Golgi-specific protein modification and vacuolar protein sorting events defined in a yeast *sec18(NSF)* mutant. J. Cell Biol. *114*, 207–218.

Guthrie, C., and Fink, G. (eds.) (1991). Guide to yeast genetics and molecular biology. Methods Enzymol. *194*, 3–38.

Haarer, B.K., Corbett, A., Kweon, Y., Petzold, A.S., Silver, P., and Brown, S.S. (1996). SEC3 mutations are synthetically lethal with profilin mutations and cause defects in diploid-specific bud-site selection. Genetics *144*, 495–510.

Harsay, E., and Bretscher, A. (1995). Parallel secretory pathways to the cell surface in yeast. J. Cell Biol. *131*, 297–310.

Holtzman, D., Yang, S., and Drubin, D. (1993). Synthetic lethal interactions identify two novel genes, *SLA1* and *SLA2*, that control membrane cytoskeleton assembly in *Saccharomyces cerevisiae*. J. Cell Biol. *122*, 635–644.

Jedd, G., Richardson, C., Litt, R., and Segev, N. (1995). The Ypt1 GTPase is essential for the first two steps of the yeast secretory pathway. J. Cell Biol. *131*, 583–590.

Kaiser, C., Michaelis, S., and Mitchell, A. (1994). Methods in Yeast Genetics, Cold Spring Harbor, NY: Cold Spring Harbor Laboratory Press.

Kaiser, C., and Schekman, R. (1990). Distinct sets of *SEC* genes govern transport vesicle formation and fusion early in the secretory pathway. Cell *61*, 723–733.

Kilmartin, J., and Adams, A.E.M. (1984). Structural rearrangements of tubulin and actin during the cell cycle of the yeast Saccharomyces. J. Cell Biol. *98*, 922–933.

Kubler, E., and Riezman, H. (1993). Actin and fimbrin are required for the internalization step of endocytosis in yeast. EMBO J. *12*, 2855–2862.

Lillie, S., and Brown, S. (1994). Immunofluoresence localization of the unconventional myosin, Myo2p, and the putative kinesin-related protein, Smy1p, to the same regions of polarized growth in *Saccharomyces cerevisiae*. J. Cell Biol. *125*:825–842.

Matile, P., Moor, H., and Robinow, C.F. (1969). Yeast cytology. In: The Yeasts, vol. 1, ed. A.H. Rose, and J.S. Harrison, New York: Academic Press, 219–302.

Mulholland, J., Preuss, D., Moon, A., Wong, A., Drubin, D., and Botstein, D. (1994). Ultrastructure of the Yeast Cytoskeleton and its association with the plasma membrane. J. Cell Biol. *125*, 381–391.

Munn, A., and Riezman, H. (1994). Endocytosis is required for the growth of vacuolar H(+)-ATPase-defective yeast: identification of six new *END* genes. J. Cell Biol. *127*, 373–386.

Munn, A., Stevenson, B., Geli, I., and Riezman, H. (1995). *end5*, *end6*, and *end7*: mutations that cause actin delocalization and block the internalization step of endocytosis in *Saccharomyces cerevisiae*. Mol. Biol. Cell *6*, 1721–1742.

Na, S., Hincapie, M., McCusker, J., and Haber, J. (1995). *MOP2* (*SLA2*) affects the abundance of the plasma membrane H^+-ATPase of *Saccharomyces cerevisiae*. J. Biol. Chem. *270*, 6815–6823.

Novick, P., and Botstein, D. (1985). Phenotypic analysis of temperature-sensitive yeast actin mutants. Cell *40*, 405–416.

Novick, P., Ferro, S., and Schekman, R. (1981). Order of events in the yeast secretory pathway. Cell *25*, 461–469.

Novick, P., Field, C., and Schekman, R. (1980). Identification of 23 complementation groups required for post-translational events in the yeast secretory pathway. Cell *21*, 205–215.

Preuss, D., Mulholland, J., Franzusoff, A., Segev, N., and Botstein, D. (1992). Characterization of the *Saccharomyces* Golgi complex through the cell cycle by immunoelectron microscopy. Mol. Biol. Cell *3*, 789–803.

Pringle, J.R., Preston, R.A., Adams, A., Streans, T., Drubin, D., Haarer, B., and Jones, E. (1989). Fluorescence microscopy for yeast. Methods Cell Biol. *31*, 357–435.

Raths, S., Rohrer, J., Crausaz, F., and Riezman, H. (1993). *end3* and *end4*, two mutants defective in receptor-mediated and fluid-phase endocytosis in *Saccharomyces cerevisiae*. J. Cell Biol. *120*, 55–65.

Read, E., Okamura, H., and Drubin, D. (1992). Actin- and tubulin-dependent functions during *Saccharomyces cerevisiae* mating projection formation. Mol. Biol. Cell *3*, 429–444.

Salminen, A., and Novick, P. (1987). A *ras*-like protein is required for a post-Golgi event in yeast secretion. Cell *49*, 527–538.

Schimmoller, F., Singer-Krueger, B., Schroeder, S., Krueger, U., Barlowe, C., and Riezman, H. (1995). The absence of Emp24p, a component of ER-derived COPII-coated vesicles, causes a defect in transport of selected proteins to the Golgi. EMBO J. *14*, 1329–1339.

Schmitt, H.D., Puzicha, M., and Gallwitz, D. (1988). Study of a temperature-sensitive mutant of the *ras*-related *YPT1* gene product in yeast suggests a role in the regulation of intracellular calcium. Cell *53*, 635–647.

Schmitt, H., Wagner, P., Ptaff, E., and Gallwitz, D. (1986). A *ras*-like protein is required for a post-Golgi event in yeast secretion. Cell *49*, 527–538.

Segev. N., and Botstein, D. (1987). The *ras*-like yeast YPT1 gene is itself essential for growth, sporulation, and stravation response. Mol. Cell. Biol. *7*, 2367–2377.

Segev, N., Mulholland, J., and Botstein, D. (1988). The yeast GTP-binding YPT1 protein and a mammalian counterpart are associated with the secretion machinery. Cell *52*, 915–924.

Sprague, G., Jr. (1991). Assay of yeast mating reaction. In: Guide to yeast genetics and molecular biology, ed. C. Guthrie and G. Fink, Methods Enzymol. *194*, 77–93.

Walworth, N., Brennwald, P., Kabcenell, A., Garrett, M., and Novick, P. (1992). Hydrolysis of GTP by Sec4 protein plays an important role in vesicular transport and is stimulated by a GTPase-activating protein in *Saccharomyces cerevisiae*. Mol. Cell. Biol. *12*, 2017–2028.

Welch, M., Holtzman, D., and Drubin, D. (1994). The yeast actin cytoskeleton. Curr. Opin. Cell Biol. *6*, 110–119.

Wright, R., and Rine, J. (1989). Transmission electron microscopy and immunocytochemical studies of yeast: analysis of HMG-CoA reductase overproduction by electron microscopy. Methods Cell Biol. *31*, 473–512.